

THE IDENTIFICATION OF RESIDUES CRITICAL IN THE EXTRACELLULAR  
DOMAIN OF THE BETA SUBUNIT OF EPITHELIAL SODIUM CHANNELS

by

Taylor Dismuke, B.S.

A thesis submitted to the Graduate Council of  
Texas State University in partial fulfillment  
of the requirements for the degree of  
Master of Science  
with a Major in Biochemistry  
May 2017

Committee Members:

Rachell Booth, Chair

Karen Lewis

Wendi David

**COPYRIGHT**

By

Taylor Dismuke

2017

## **FAIR USE AND AUTHOR'S PERMISSION STATEMENT**

### **Fair Use**

This work is protected by the Copyright Laws of the United States (Public Law 94-553, section 107). Consistent with fair use as defined in the Copyright Laws, brief quotations from this material are allowed with proper acknowledgement. Use of this material for financial gain without the author's express written permission is not allowed.

### **Duplication Permission**

As the copyright holder of this work I, Taylor Dismuke, authorize duplication of this work, in whole or in part, for educational or scholarly purposes only.

## **DEDICATION**

I dedicate this work to my guardian angel, Charlene Dismuke.

## **ACKNOWLEDGEMENTS**

This work would not have been possible without the financial support of the Bridge to Doctoral program and the thesis support fellowship. I am especially indebted to Drs. Walter, Oyabobi, and Blake who have been in my corner supporting and pushing me to become a better scientist. The bridge program provided not only the financial support for me to focus on my research but the developmental lessons in becoming a better professional scientist. Thanks is also warranted for my lab mate, Toyosi Adewunmi, for being a strong support system in my time of need.

I would like to give thanks to Dr. Rachell Booth, my committee chair and advisor in the Bridge Doctoral program. It has been a pleasure to work with you throughout this project and have your support. From the scientific edits to the advice on my career, you have been essential throughout my evolution as a scientist. Also, I would like to extend my thanks to Drs. Wendi David and Karen Lewis for being on my committee. Both, have pushed me to remain critical about my project.

Nobody had a greater role in my success than my family. I would like to thank my parents for listening to me and encouraging me in my dark times. When I thought I wanted to give up it was both of my parents who kept me focused through the storm. To my siblings, when I was down you both gave me the humor I needed to pick up my spirits. I am grateful to have all the following be a part of my journey at Texas State University and I am excited about what the future has in store for me.

## TABLE OF CONTENTS

	<b>Page</b>
ACKNOWLEDGEMENTS .....	v
LIST OF TABLES .....	vii
LIST OF FIGURES .....	viii
CHAPTER	
I. INTRODUCTION AND LITERATURE REVIEW .....	1
II. MATERIALS AND METHODS .....	12
III. RESEARCH RESULTS AND DISCUSSION .....	22
IV. CONCLUSIONS .....	51
WORKS CITED .....	53

## LIST OF TABLES

<b>Table</b>	<b>Page</b>
1. Primers for Error Prone Polymerase Chain Reaction of Beta and Gamma ENaC .....	13
2. Endonucleases and Restriction Sites.....	15
3. Primers Used for PCR amplification of Isolated Yeast Plasmid .....	18
4. Primers Used for Sequence Analysis .....	19
5. Characterization of Nucleic Acid Changes in Beta Mutant 1-4 .....	46
6. Characterization of Amino Acid Changes in Beta Mutant 1 .....	48

## LIST OF FIGURES

<b>Figures</b>	<b>Page</b>
1. Schematic of sodium and water reabsorption in nephron.....	3
2. Structural depiction of ENaC.....	5
3. Nedd4-2 aids in downregulation of voltage-gate channels.....	7
4. ENaC Regulation by Extrinsic and Intrinsic Factors.....	10
5. Horizontal Electrophoresis of epPCR reactions of pESC-LEU $\beta$ -ENaC and pESC-LEU $\gamma$ -ENaC.....	23
6. Schematic of pESC-LEU expression vector.....	25
7. Schematic depiction of recombination of pESC-LEU $\beta/\gamma$ ENaC with mutated region.....	26
8. Horizontal Electrophoresis of Digestion of pESC-LEU $\beta\gamma$ ENaC.....	27
9. Digestion of pESC-LEU $\beta\gamma$ ENaC with ZraI and SexAI.....	28
10. Gel Extraction of Digested pESC-LEU $\beta\gamma$ WT.....	29
11. Survival Pronging Dilution Assay of Beta mutants in Heterotrimeric Complex.....	32
12. Immunoblot of $\beta$ -ENaC mutants using anti-beta antibody.....	34
13. Figure 13: Digestion of pESC-LEU $\beta/\gamma$ ENaC WT and pYES2NTA $\alpha$ ENaC WT.....	36
14. Double Digestion of Beta mutant 2 samples with XhoI and NheI.....	37
15. Double Digestion of Beta mutant 3 samples with XhoI and NheI.....	38
16. Single Digestion of Beta mutant 4 samples with XhoI.....	39
17. Double Digestion of Beta mutant 1 samples with XhoI and NheI.....	41
18. High Fidelity PCR amplification of SCNN1B in Beta mutant 1 samples.....	42
19. Multiple DNA Sequence Alignment of Beta-ENaC.....	46
20. Multiple Amino Acid Sequence Alignment of Beta-ENaC.....	47

21. Mutations in Beta mutant 1 in the Extracellular Loop Secondary	
Structure .....	49
22. Confocal Microscopy of Beta mutant 1 in BY4742 cells .....	50

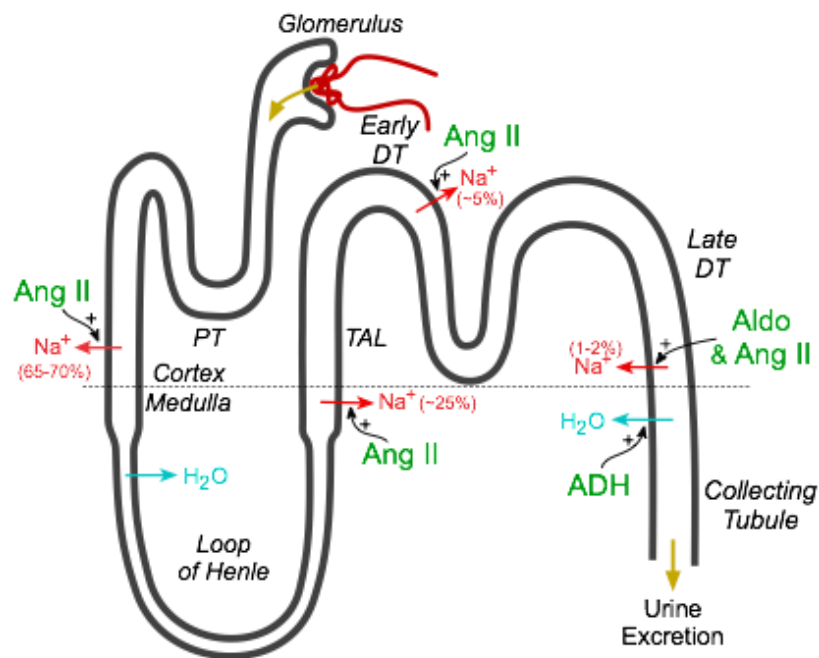
## I. INTRODUCTION AND LITERATURE REVIEW

The composition of salt (i.e. NaCl) in human diets impacts sodium ion levels in biological systems. For example, significant increase in salt intake can lead to osteoporosis, kidney stones, and/or hypertension (1-3). Osteoporosis is a skeletal disease that can lead to the weakening of bones resulting from the excretion of calcium due to a significant increase in the intake of sodium (1, 2). Increased sodium levels can also cause the kidneys to excrete more calcium into the urine where the calcium precipitates to form kidney stones (1-3). In addition, elevated sodium levels can lead to an increase on sodium reabsorption rates in the kidney (1-3). When sodium is transported across the kidney cells water reabsorption follows the transport of ions (1-3). As more ions are transported into the blood this results in an increase volume of water in the blood. Since sodium reabsorption is coordinated to water reabsorption, when the volume of water increases severely in the blood it can lead to hypertension or high blood pressure (1, 4). Untreated blood pressure can give rise to heart disease, kidney disease, stroke, atherosclerosis, and death (1-3, 5). With cardiovascular disease making up 31% all global deaths, clearly demonstrates a need for further advances in therapeutic targeting of macromolecules that aid in sodium transport (5).

Osmoregulation is the process by which the body regulates organismal systemic water levels (2). This regulation aids in the dilution or concentration of bodily fluids, such as blood and urine. Osmoregulation can be controlled, in part, by ion channels that specialize in the reabsorption of specific ions and solutes within organs, especially the kidneys (2). The kidneys' primary function is to maintain electrolyte and pH balance in the blood (1-4).

The blood travels through the circulatory system from arteries carrying and collecting ions and solutes that the body needs until it reaches the kidneys for filtration. When the blood from the renal artery first reaches the kidney, it is filtered through the glomerulus before entrance into the nephron (3) (Fig 1). The filtrate then travels through the proximal collecting tubules where a large percentage of sodium reabsorption takes place. Specialized epithelial cells in the tubular wall are used to sense the presence of sodium and other ions in the filtrate. In the presence of sodium ions, the tubule cells release an enzyme, called renin, which catalyzes the reaction of angiotensinogen to angiotensin I (3). An angiotensin-converting enzyme (ACE) converts angiotensin I to angiotensin II (2, 3). Angiotensin II stimulates more sodium reabsorption across the tubule walls. When the filtrate reaches the last portion of the distal tubule, sodium reabsorption is stimulated by both angiotensin II and aldosterone (2-4) (Fig 1). Aldosterone, in turn, regulates the transport of sodium ions from the tubular fluid into the renal interstitium compartment. The renal interstitium is a compartment situated between the epithelial cells and nutritive capillaries where reabsorption and secretion of fluids occurs where an exchange between tubular and vascular structures occurs (1, 3-4). Aldosterone shares a physiological relationship to renin and angiotensin because both hormones promote sodium reabsorption. These three hormones form a renin-aldosterone-angiotensin system (RAAS) that collectively regulates sodium reabsorption in the kidneys (4). Also, when there needs to be a cease to sodium reabsorption the hormones are removed to cease sodium transport across the epithelial kidney cells. Sodium transport is not the only pathway that regulates blood pressure. When sodium is transported across kidney wall to the lumen of the renal vein water is transported through

aquaporins (1-3). The volume of water transported back into the blood is dependent on the concentration of transported sodium ions. Water transport coincides with sodium reabsorption and is stimulated by an antidiuretic hormone (ADH). ADH aids in the regulation of water permeability in the proximal and collecting tubules (Fig 1). The combined regulatory response to the RAAS system and ADH in the kidney results in sodium and water reabsorption (4). The remaining filtrate in the kidney is excreted in the form of urine (Fig 1).



Abbreviations: PT, proximal tubule; TAL, thick ascending limb of loop of Henle; DT, distal tubule; Ang II, angiotensin II; Aldo, aldosterone

**Figure 1: Schematic of sodium and water reabsorption in a nephron.** This is a depiction of the transport of sodium and water in a nephron. While the blood filtrate enters the nephron at the glomerulus it exits the collecting tubule in the form of urine. The recruitment of different hormones stimulate sodium and water reabsorption (6)

Ion channels are transmembrane proteins that can transport ions like sodium and calcium across the cell membrane. There are several types of specific, tightly regulated protein channels found in the membranes of tubules cells. The transport function of protein channels can be modulated by conformational changes from an open state to a closed state (i.e. gating). The gating of channels can be activated by voltage, binding of a ligand, and/or mechanical changes in surface tension of the membrane. The protein channel modulating sodium reabsorption in the distal tubules and collecting duct cells of the nephrons is the epithelial sodium channel (ENaC).

ENaC belongs to the ENaC/Degenerin super family which share structural and functional domains that are involved in the activity and pore formation (6-25). ENaC is a membrane-bound ion channel that mediates sodium reabsorption in various tissues including kidney, colon, lung, and sweat glands. Because of the channel pore size, ENaC favors the transport of sodium ions over other cations, with the exception of lithium (6). Lithium and sodium atomic radii are close in size of proving more difficult to distinguish two (7). One member of this family is the acid-sensing ion channels (ASIC), which are involved in pain sensation (6-26). Members of the Degenerin family share structural characteristics that are common to this family. The structure of ASIC (from chicken) has served as a model for the understanding of ENaC structure.

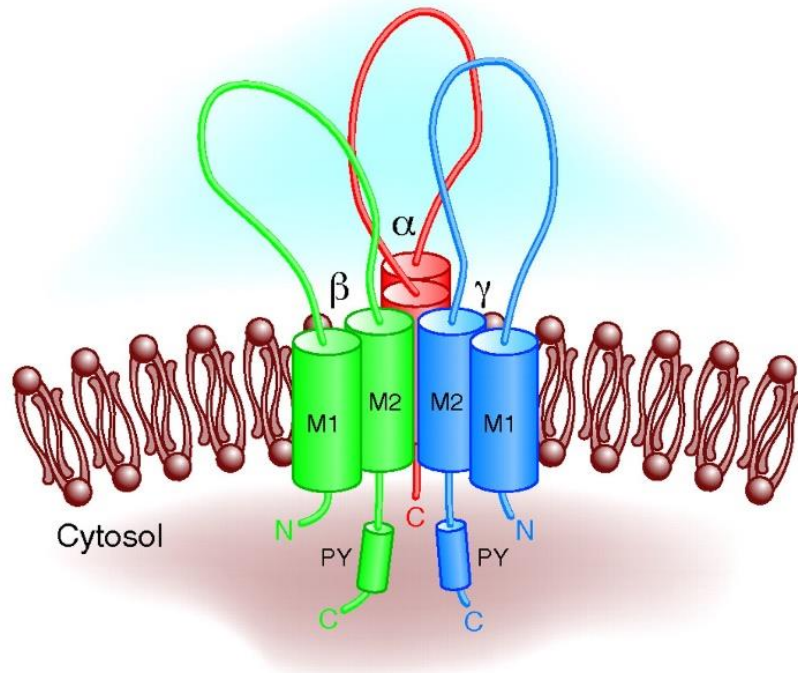


**Figure 2: Structural depiction of ENaC.** This diagram is a proposed structural depiction of ENaC. ENaC is a transmembrane protein made up of seemingly three homologous subunits:  $\alpha$ ,  $\beta$ , and  $\gamma$ . Each subunit contains two transmembrane domains addressed as M1 and M2. The cytosolic region of ENaC contains both the N-termini and C-termini of each subunit. On both the  $\beta$  and  $\gamma$  subunit C-termini ends there is an incorporated PY motif. The extracellular domain contains a large extracellular loop on each subunit. (8)

ENaC is a heterotrimeric protein (Fig 2). The homologous subunits of ENaC in the kidney are the alpha ( $\alpha$ ), beta ( $\beta$ ) and gamma ( $\gamma$ ) subunits (Fig 2). Each subunit has two membrane-spanning domains, a large extracellular loop, and a short intracellular N-termini and C-termini (Fig 2). ENaC is made up of various combinations of the alpha, beta, and gamma subunits (ie.  $\alpha\beta\alpha$ ENaC  $\alpha\alpha\alpha$ ENaC,  $\alpha\beta\gamma$ ENaC) (6-9). Two of the subunits,  $\beta$  and  $\gamma$ , are structurally different from  $\alpha$  subunit. The  $\beta$  and  $\gamma$  subunit cytoplasmic domains contain a “PY” motif on their C-termini ends (Fig 2). The PY motif

allows for the interaction with proteins that contain a WW domain (9). Schild et al. showed that deletion of the PY motif resulted in an increase of channel activity (9). The PY motif aids in the repression of ENaC localization in the membrane (9). Suggesting that cleavage of an inhibitory peptide in the finger domain on the  $\alpha$  subunit of ENaC results in an active conformation of the channel, Shobair et al. showed that inter-subunit interactions aid in the activation of the ENaC channel (11). Computational studies (discrete molecular dynamic simulations) were used to predict differences in interactions between the subunits and their effect on the channel pore. Using site-directed mutagenesis to eliminate interactions between the subunits at  $\alpha$ Arg493 and  $\gamma$ Glu-348, the disruption of this interaction fully activated the  $\alpha$ W493R (gain of function mutation) in ENaC. A gain of function mutation on ENaC results in the channel having an increased presence on the membrane for activity. After disrupting interacting residues between the subunits that were aiding in the self-inhibition of ENaC, the  $\alpha$ W493R mutant increased intersubunit interaction promoting channel activity (11, 12).

The alpha subunit is unique in that it can form functional channels alone (8-24). While beta and gamma ENaC subunits cannot replicate this same feature, the most functional form of ENaC in nature is the heterotrimeric complex with all three subunits (13). This implicates beta and gamma subunits as accessory subunits that aid in the regulation of ENaC. There have been several reports of critical intracellular domains of  $\beta$ - and  $\gamma$ - ENaC subunits that aid in regulation. Mukherjee et al. reported previously that palmitoylation of the cytoplasmic regions of the  $\beta$  and  $\gamma$  subunit plays a role in channel gating by stabilizing the open state of the channel (13). Mukherjee et al. created mutations on the cytoplasmic cysteine residues of the  $\beta$ - and  $\gamma$ - subunits to determine if

there was reduced ENaC activity being that palmitoylation would not take place (13). Both mutations resulted in a decrease of present ENaC on the membrane thereby confirming that palmitoylation on the  $\beta$  and  $\gamma$  subunit plays a role in ENaC membrane trafficking. Since the loss of activity in the mutant  $\gamma$  subunit was greater than the mutant  $\beta$  subunit, palmitoylation of the  $\gamma$  subunit was perceived to have the greatest effect on membrane localization (13).

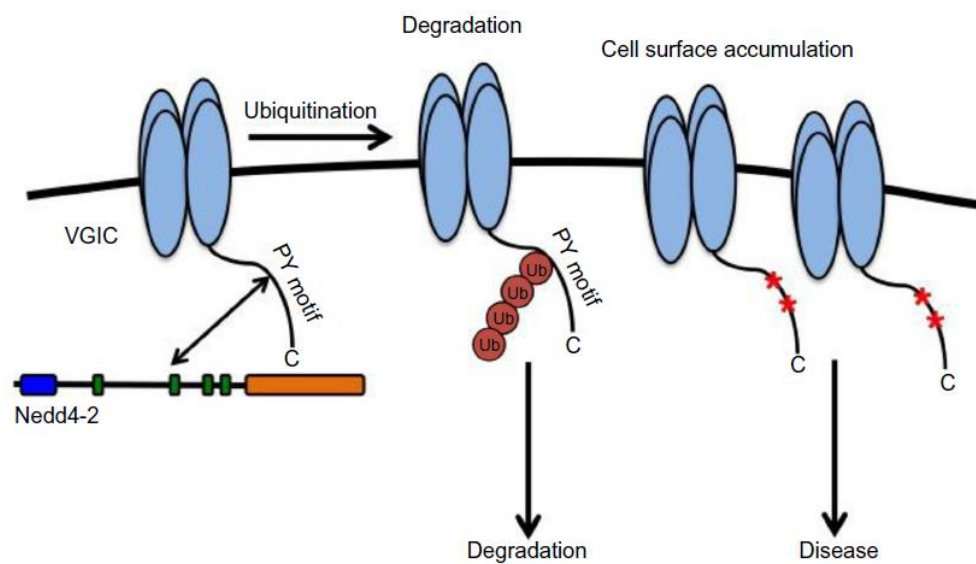


**Figure 3: Nedd4-2 aids in the downregulation of voltage-gate channels.** This is a schematic representation of Nedd4-2's regulation of voltage-gated channels through ubiquitination. Nedd4-2 signals for ubiquitination of the PY-motif on the C-termini ends of the channel. The ubiquitination of the channel signals for lysosomal or proteasomal degradation. Without the signaling of the ubiquitination the channels will not be targeted for degradation resulting in cell surface accumulation (14)

The PY motif on the  $\beta$  and  $\gamma$  subunit are known to contain sites for ubiquitination.

One enzyme with ubiquitination activity is called NEDD 4, also known as neural

precursor cell expressed developmentally down-regulated protein 4. The neural precursor cell expressed developmentally down-regulated protein (NEDD4) is a ligase that carries out ubiquitination of proteins which in turns targets ENaC for lysosomal or proteasomal degradation (14, 15) (Fig 3). As shown by Dinudom et al, the C-termini of the  $\beta$  and  $\gamma$  subunits contain residues that aid in the downregulation of ENaC by ubiquitination (16). This was determined by whole-cell patch clamp methods using synthetic peptides of the C-termini ends of the  $\alpha$ -,  $\beta$ -, and  $\gamma$ - subunits of ENaC and fusion proteins. This study expressed that the C-termini ends of the  $\beta$ - and  $\gamma$ - subunit, not including the  $\alpha$ - subunit, contained peptides that aided in the inhibition of ENaC by containing regions for ubiquitination (16). Ubiquitination of ENaC results in the translocation of the channel from the apical membrane into the cytosol for lysosomal or proteasomal degradation (14-16) (Fig 3, Fig 4). Staub et al. reported a correlation between ubiquitination and the number of functional channels at the cell surface (17). Mutations of N-termini lysine residues in  $\gamma$  ENaC lead to a decrease in ubiquitination and an increase in ENaC activity in sodium reabsorption providing direct evidence of  $\gamma$ ENaC's role in ubiquitination-mediated regulation of channel stability (17).

ENaC is also regulated in the kidney by hormonal control and several external factors (14, 15, and 18) (Fig. 4). Butterworth reported that aldosterone was shown to rapidly distribute ENaC from intracellular cytoplasmic regions in the cell to the apical membranes of nephron cells (18). Hormonal control allows for the effects to be greater in the body and last longer in the organismal system. Fridnt et al. conducted a single channel analysis of ENaC on rats placed on a salt-restricted diets and showed that the increase of ENaC activity correlated with the number of channels on the apical surface

after a short term exposure to aldosterone (18). Their studies suggested that the hormonal response to dietary changes results in the mobilization of ENaC between the cytosol and the apical surface membrane. In addition, aldosterone increases  $\alpha$ ENaC channel mRNA production (18-20).

ENaC can also be regulated by several external factors. One external factor that inhibits ENaC activity is potassium-sparing diuretics (such as amiloride). Amiloride is a drug used in the treatment of hypertension and congestive heart failure. Amiloride mechanism of inhibition is the direct blockage of ENaC pore thereby inhibiting sodium reabsorption (6, 8). A second extrinsic factor that regulates ENaC is activation by proteolytic cleavage (Fig 4). Haertis et al reported two cleavage sites in the extracellular loop of the  $\gamma$  subunit of human ENaC that are critical in the proteolytic activation by a protease (21). The mutation of these cleavage sites resulted in a decrease in channel activity (21). The extracellular loop acts as another point of regulation on the ENaC channel (9, 21)

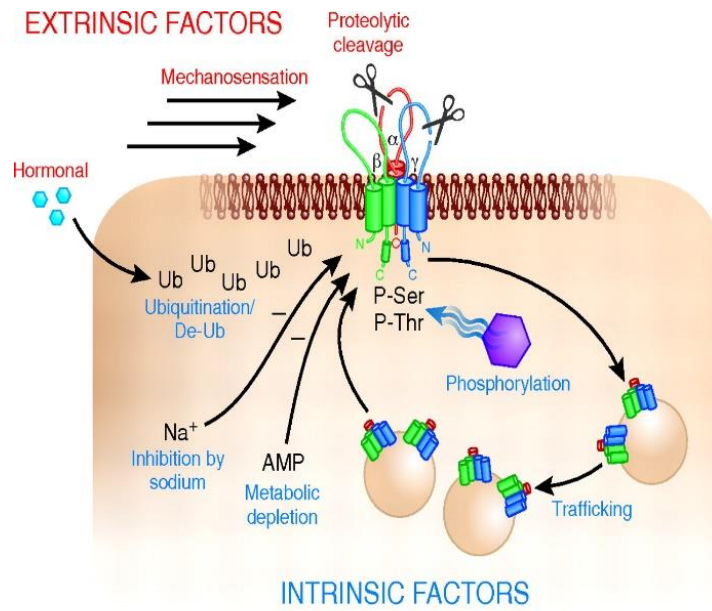


**Figure 4: ENaC Regulation by Extrinsic and Intrinsic Factors.** This diagram is an overview of extrinsic and intrinsic factors that aid in the regulation of ENaC. Ubiquitination of ENaC results in lysosomal or proteasomal degradation. ENaC can undergo self-inhibition in response to intracellular sodium levels. Proteolytic cleavage of the extracellular loop activates ENaC. Responses to mechanosensation, AMP concentrations, and phosphorylation also aid in the regulation of ENaC (15).

The rate-limiting step of trans-epithelial Na<sup>+</sup> reabsorption in the kidneys is the apical Na<sup>+</sup> entry through ENaC (5-24). Dysfunction of ENaC is linked to various cardiovascular diseases such as Liddle's syndrome (gain-of-function mutations, severe hypertension) and pseudohypoaldosteronism (loss-of-function mutations, severe hypotension) (22-24). Yang et al. reported that patients with Liddle's syndrome shared a frameshift mutation on the  $\beta$  subunit that resulted in a truncated protein (22). Edelheit et al. reported mutations on the carboxyl-terminal domain of the  $\beta$  subunit of ENaC produced a truncated protein which was previously correlated with Liddle's syndrome (23). In Edelheit et al. studies, mutant forms of the  $\beta$ - subunit were generated using site-

directed mutagenesis and then injected into *Xenopus* oocytes with normal and mutant cloned cDNAs to observe channel activity (20). Those mutations had two effects: (1) a gain of function of the ENaC or (2) inhibition of the ubiquitination regulation (20). Kucher et al. reported that a mutation of any of the three subunits of ENaC on the conserved glycine residues near the NH<sub>2</sub>-terminus resulted in a loss of function, which is a common mutation amongst patients with some forms of pseudohypoaldosteronism (PHA-1) (24, 25).

Since the intracellular domains of ENaC have been well studied and studies that characterize the importance of the extracellular domains of ENaC are just emerging, the Booth laboratory is focused on studying residues in the extracellular domain that are critical to ENaC function (26-28). A novel yeast screen was developed by Raquel Ybanez to screen the function (i.e. sodium ion transport) of ENaC, where a survival dilution assay is used (26). This screen is used to identify preliminary residues are critical for ENaC function (26-28).

The following project focused on characterizing the functional role and important extracellular domains of beta and gamma ENaC subunits from *Mus musculus*. Comprehension of the structure-function relationship of ENaC subunits will give better insight to their contributions to the heterotrimeric complex in native systems. Better understanding of sodium transport in the human body will give rise to better efforts in the treatment of cardiovascular disease.

## II. MATERIALS AND METHODS

All centrifugation steps were carried out by the Eppendorf Centrifuge 5424 or Sorvall™ LYNX 6000™ Centrifuge (ThermoFisher scientific). Incubations in the water bath were with the Baxter-Durabath™ Water Bath. Polymerase chain reactions were analyzed on a T100™ Thermal Cycler (Biorad Laboratories). Purified DNA was quantified using the Nanodrop 2000 (ThermoFisher scientific). All horizontal and vertical gel electrophoresis was analyzed with the Electrophoresis Power Supply 601 (Amersham Pharmacia Biotech). Protein optical density was measured during the BCA protocol using the iMark™ Microplate Reader (Biorad Laboratories). Culture optical density was measured with Smartspec™ Plus Spectrophotometer (Biorad laboratories). All primers were made at the Integrated DNA technologies laboratories and sent in 100 μM concentrations and stored at -4°C. All gels and blots were visualized on the Molecular Imager Chemi-Doc™ XRS + Imaging System (Bio rad laboratories). Light microscope used was the CKX41 Culture Microscope (Olympus Life Science).

### **Error-Prone PCR of pESC-LEU Beta and pESC-LEU Gamma Plasmid Vectors**

The error-prone PCR reaction included: 3 mM MgCl<sub>2</sub>, 1X Standard Taq Buffer (New England Biolabs), 2 mM dNTPs, 1 mM of selected primers (Table 1), 5 units of Taq DNA polymerase, and ddH<sub>2</sub>O to bring the final reaction volume to 50 μL. The PCR reaction was carried out under these conditions: 94°C for 1 minute, 60°C for 30 seconds, 55°C for 30 seconds, and 72° C for minutes. These conditions analyzed for 25 repeated cycles and extended for 7 minutes at 72° C. Reaction was analyzed using horizontal gel

electrophoresis and cleaned up using the Zymo Research DNA Clean and Concentrator™-5 Kit. Purified PCR products were quantified on Nanodrop.

**Table 1: Primers for Error Prone Polymerase Chain Reaction of Beta and Gamma ENaC.** All primers had a final concentration of 1 $\mu$ M in each reaction.

Primer Name	Primer Sequence
UP BmENaC Random	5'-CCAGGACCCTGAACTTTACC-3'
DN BmENaC Random	5'-CTGGCAGGTTTAGATAGCAATAGGC-3'
UP GmENaC Random	5'-AAGATGTTCTAGACAGTACACCTCG-3'
DN GmENaC Random	5'-CAGCTGGTAGTAGCAATACATGG-3'

### Plasmid Isolation from *E. coli*

*E. coli* transformed with plasmid (pESC-LEU beta/gamma ENaC or pYES2NTA alpha ENaC) was grown overnight in 5 mL of LB Broth with the addition of 100  $\mu$ g/mL ampicillin at 37°C under continuous shaking. A volume (3-4mL) of the overnight culture was spun down at 8000g and the supernatant was discarded. The DNA was isolated using the QIAprep Spin Miniprep Kit. Buffer P1 was added to the pellet to resuspend the cells. Buffer P2 was added to the volume, inverted gently 4-6 times, and incubated at room temperature to lyse cells. Buffer N3 was added to neutralize the lysis reaction. Solution was spun down at 10000g for 10 minutes. Supernatant was applied to a spin column and spun down for 8000g for sixty seconds. The flowthrough was discarded and the column was washed with wash buffer. DNA was eluted with 50  $\mu$ L of sterile water and quantified using the Nanodrop.

## **Horizontal Gel Electrophoresis**

For horizontal gel electrophoresis, 1 % w/v agarose slab gels were prepared using 1X TAE Buffer (40 mM Tris-base, pH 8, 20 mM acetic acid, 1 mM EDTA) with the final volume of 50 mL. Gels were suspended in 1X TAE buffer and analyzed on an electrophoresis apparatus at 100 V-110V for 1-1.25 hours.

## **High Efficiency transformation Using *E. coli* 2925 competent cells**

*E. coli* 2925 cells were thawed on ice for 10 minutes. Five micrograms of pESC-LEU  $\beta/\gamma$  was added to the cells and incubated on ice for 30 minutes. Cells were heat-shocked at 42° C for 30 seconds and then incubated on ice for 5 minutes. LB Broth (950 $\mu$ L) was added to cells at 37° C for 1 hour with continuous shaking. The cells were spread on LB Agar/100  $\mu$ g/mL ampicillin plates and incubated overnight at 37° C. Individual colonies were picked with a sterile toothpick and grown overnight in 5 mL of LB/AMP Broth.

## **Digestion of plasmid vector using endonucleases**

Digestion reactions varied contained plasmid DNA, 1X of Cutsmart Buffer, 1X of Bovine Serum Albumin, 2 units of endonuclease (Table 2), and sterile water to a final volume of 30  $\mu$ L. The digestion reaction was incubated at 37 ° C in a water bath and stopped using 1X Endostop Buffer. The products were analyzed by horizontal gel electrophoresis.

**Table 2: Endonucleases and Restriction Sites:** All restriction enzymes were from New England Biolabs.

Endonuclease	Restriction Site
ZraI	5'-GAC   GTC-3'
SexAI	5'-A   CCWGGT-3'
NheI	5'-G   CTAGC-3'
XhoI	5'-C   TCCGAG-3'

### **Gel Extraction**

Gel extraction of DNA fragments was carried out using the standard protocol from the QIAEX II Gel Extraction Kit. DNA fragments of interest were first excised while visualized on a UV light transilluminator for short periods of time to reduce DNA damage from UV exposure. Eluted DNA was cleaned up using the DNA Clean Concentrator Kit using the manufacturer's protocol and quantified using the Nanodrop.

### **Transformation of isolated plasmid and purified PCR into BY4742 yeast cells**

Transformation of multiple plasmids in yeast had to be carried out in a step wise fashion with pYES2NTA- $\alpha$  being transformed first and grown on glu-ura (1 % w/v yeast extract, 2 % w/v BactoPeptone, 2.5 % w/v BactoAgar, 0.2 % w/v adenine, 1 % w/v leucine and 2 % w/v glucose) selective media plates. The pESC-LEU Beta plasmid and purified epPCR product were co-transformed into BY4742 yeast cells containing the pYES2NTA-alpha ENaC using the lithium acetate transformation protocol.

BY4742/pYES2NTA-alpha ENaC yeast cells were cultured overnight at 30°C in 10 mL

of the selective media glu-ura (0.67% w/v yeast nitrogen base, 0.14% w/v yeast synthetic drop-out media, 0.5% w/v tryptophan, 0.2% w/v histidine, 1% leucine and 2% w/v glucose). Overnight culture (1 mL) was spun down on an Eppendorf™ Centrifuge 5254 at 12000g for 30 seconds and the supernatant was discarded. In the following order: 33% PEG 3350, 0.1 M LiAc, 0.28 ng/mL salmon sperm DNA, 2.8 mg/mL beta mercaptoethanol, >1000 ng/μL of DNA samples were mixed. ddH<sub>2</sub>O was added to bring the final reaction volume to 360 μL. The reaction mixtures were vortexed for 1 minute, incubated for 20 minutes in a 42°C water bath, and centrifuged at 3000g for 2 minutes. The pellet was resuspended in 200μL of ddH<sub>2</sub>O. The transformant reaction (150 μL) was plated on the selective media glu-ura-leu (3 % w/v Bactoagar, 0.67 % w/v yeast nitrogen base, 0.14 % w/v yeast synthetic drop-out media, 0.5 % w/v tryptophan, 0.2 % w/v histidine, and 2 % w/v glucose) plates and incubated for 3-5 days at 30° C. Yeast cells carrying two plasmids were grown for 4-6 days.

### **Salt-Sensitivity Assay**

Salt-sensitivity assay for yeast cells was previously described (27). Fresh patch plates of yeast cells were grown on glu-ura-leu (1 % w/v yeast extract, 2 % w/v BactoPeptone, 2.5 % BactoAgar w/v, 0.2 % w/v adenine, and 2 % w/v glucose) plates overnight at 30 ° C. From patch plates a pellet (i.e. size of nail head) was scraped with a sterile toothpick and resuspended in 500 μL of sterile ddH<sub>2</sub>O. A 40-fold dilution from the previous made stock of yeast cells was sonicated at 30 amps for 10 seconds using a VIBRA cell probe sonicator. The average number of cells were counted using a hemocytometer with the CKX41 Culture Microscope (Olympus Life Science). Cells were approximately calculated and added to the first well with the addition of ddH<sub>2</sub>O to bring a

volume of 220  $\mu$ L. The cells were diluted across the five remaining wells resulting in a 5-fold serial dilution. Cells were spotted onto selective media plates both glu-ura-leu//+/- 0.5M NaCl (1 % w/v yeast extract, 2 % w/v BactoPeptone, 2.5 % BactoAgar w/v, 0.2 % w/v adenine, and 2 % w/v glucose) and gal-ura-leu// +/- 0.5M NaCl (1 % w/v yeast extract, 2 % w/v BactoPeptone, 2.5 % BactoAgar w/v, 0.2 % w/v adenine, and 1 % w/v galactose). Selective media plates were incubated at 30° C for 3-5 days for glucose plates and 5-8 days for galactose plates.

### **Yeast Plasmid Isolation**

One milliliter of overnight yeast cultures was centrifuged at 3000g for 3 minutes. The pellet was resuspended in 0.01 mg/mL of zymolase, 500 mM of sodium phosphate buffer (pH 7.5), and ddH<sub>2</sub>O to bring a final volume of 1 mL. The sample was vortexed for 30 seconds and then incubated at 37° C for 1 hour. The DNA was extracted using the QIAGEN Spin Miniprep Kit standard protocol. Isolated DNA was quantified using the Nanodrop.

### **Transformation of Yeast plasmid into Top 10 *E. coli* using KCM Buffer**

Top 10 *E. coli* cells were thawed on ice for 10 minutes. One hundred microliters of cold KCM buffer was added to the cells. 0.01-0.02  $\mu$ g of yeast plasmid was added to the cells and gently mixed. Cells were incubated on ice for 15 minutes followed by room temperature (25-30° C) for 10 minutes. LB broth (900  $\mu$ L) was added to the cells. The culture was incubated with shaking for 37° C for 1 hour. Culture was spread on LB/AMP plates and incubated at 37° C overnight.

## High fidelity PCR

For high efficiency amplification, the Phusion polymerase PCR amplification protocol was used. The following was added to the PCR tube in this exact order: 1X of Phusion HCF Buffer, 0.5 mM of selected primers (Table 2), 0.2 mM of dNTPs, 0.1 ng of yeast plasmid, 1 unit of Phusion polymerase, and ddH<sub>2</sub>O to bring the final volume to 50  $\mu$ L. The thermocycler conditions for this PCR reaction was the following: 98° C for 30 seconds, 72° C for 25 seconds, and 72° C for 30 seconds for 35 cycles. The PCR product analyzed by horizontal gel electrophoresis and cleaned up using the DNA Clean and Concentrator Kit protocol.

**Table 3: Primers Used for PCR amplification of Isolated Yeast Plasmid.** All primers had a final concentration of 1 $\mu$ M in each reaction.

Primer	Primer Sequence
BmENaC pESC- LEU UP	5'-CGAACTCGAGCTTATGCCAGTGAAGAAAGTACC-3'
Mouse Beta DN	5'-GCAAGCGGCCGCCTAGATGGCCTCCACCTCACT-3'

## Sequence analysis

Mutant plasmids were sent to Quintara Biosciences (Richmond, CA) for sequencing. The plasmids and primers had a concentration of 5  $\mu$ M (Table 4).

**Table 4: Primers Used for Sequence Analysis.** Primers were selected under the notion that the following anneals to the SCNNB gene and galactose promoters on the expression vector.

Primer	Primer Sequence
Gal1Forward	5' ATTTTCGGTTTGTATTACTTC 3'
Gal1Reverse	5' GTTCTTAATACTAACATAACT 3'
Beta Internal Sequencing-Reverse	5' AATTCAGTCCCAGGGTTGGCAGAAGG 3'
Beta Internal Sequencing-Forward	5' ATGGAACTGTGTGTACCTTGCG- 3'

### Protein Isolation from Yeast Mutants

Yeast containing mutant and wildtype  $\beta$ ENaC were grown overnight in 15 mL glu-ura-leu selective media broth. A 0.4 OD<sub>600</sub> of the overnight culture was removed from the overnight cultures and spun down at 3000g for 3 minutes. The pellet were each resuspended in 3 mL of gal-ura-leu selective media broth. The resuspended culture was added to 47 mL of gal-ura-leu selective media broth and allowed to grow to an OD<sub>600</sub> of 1 for 8 hours. Optical density at 600 nm was measured using a spectrophotometer. Cells were harvested.

Yeast cells were lysed using acid-washed glass beads in RIPA buffer (150 mM NaCl, 50 mM Tris, 1% v/v Triton X-100, and 1% w/v sodium deoxcholate). Fresh protease inhibitors were added to RIPA buffer for lysis. An equal volume of lysis buffer and glass beads were added to pellet. Equal volume of glass beads was added to each pellet. Cells were vortexed in 30 second intervals for 8 minutes. Samples were incubated on ice between each vortex interval. Samples were centrifuged at 8000g for 10 minutes and the supernatant containing extracted protein was stored at -20° C.

## **Western blot of $\beta$ ENaC subunit Expression from Yeast Samples**

One hundred micrograms of extracted protein was calculated using the Pierce™ BCA Protein kit (ThermoFisher scientific) protocol for SDS-PAGE. 100  $\mu$ g of protein samples were loaded into a 7% SDS –PAGE gel at 120V for 1 hour. Using the protocol in the Transblot™ Turbo Transfer System RTA Transfer Kit (Bio Rad Laboratories) the SDS-PAGE gel was transferred onto a nitrocellulose membrane. The transfer was for 20 minutes at 20 V and 1.3A. The nitrocellulose membrane was then blocked in a 5% blocking buffer (5 % w/v dry milk, 1X TBST) for 30 minutes. The nitrocellulose membrane was washed 3 times using TBST (10% Tris-Buffered saline pH 7.4, 0.1 % v/v Tween). The membrane was then incubated with a 1:1000 dilution of 1mg/mL Rabbit anti-beta polyclonal antibody (StressMarq Biosciences, Victoria, CA) overnight at 4 ° C with shaking. The nitrocellulose membrane was washed 3 times using TBST. Then then membrane was incubated with a 1:20000 dilution of 1.0 mg/mL peroxidase-labeled affinity purified antibody to rabbit IgG (H+L) (Human Serum Absorbed) (KPL, Gaithersburg, MD) for 1 hour at 4 ° C. Again, the nitrocellulose membrane was washed 3 times using TBST. The membrane was washed a fourth time with 1X TBS and then developed using the Western Lightning® Plus-ECL kit (PerkinElmer, Inc., Waltham, MA).

## **Immunofluorescence staining for confocal microscopy**

Preparation of yeast cells for confocal microscopy was described previously (28). Overnight cultures from fresh patch plates were grown in induction media (gal-ura-leu

broth) for 2 hours and spun down at 3500g at 4° C. Cells were then fixed with a 16 % formaldehyde solution for 1 hour at room temperature. Fixed yeast cells were incubated in 1: 100 dilution of 1 mg/mL anti-c-myc peroxidase (Roche Diagnostics, Indianapolis, IN) overnight at room temperature. After slides were washed, cells were incubated in a 1: 1000 dilution of 2 mg/mL Alexaflour™ 488 goat anti-mouse IgG H+L(Life Technologies Corp., Eugene, OR) for 1 hour in the dark at room temperature. Washes after the secondary antibody were all performed in the dark. Slides were mounted with a 60 % glycerol solution and incubated for 2 hours in the dark at room temperature. Visualization of cells were carried out on the FV1000 Confocal Microscope (Olympus Life Sciences).

### III. RESULTS AND DISCUSSION

#### Random Mutagenesis of SCNN1B and SCNN1G

The identification of critical amino acid residues on the extracellular loop of  $\beta$ -ENaC was initiated by random mutagenesis of both the  $\beta$ -ENaC gene, SCNN1B, and  $\gamma$ -ENaC gene, SCNN1G. Random mutagenesis was carried out using error-prone polymerase chain reaction (PCR). Error-prone PCR was performed by altering reaction conditions that would increase the error rate of Taq polymerase. The concentrations of  $MgCl_2$  were increased to 3mM to promote the mutations along a targeted region, within the extracellular loop of  $\beta$ -ENaC. The addition of excess magnesium in PCR affects the efficiency and specificity of the polymerase. It was determined that increasing the  $Mg^{++}$  concentration from a standard of 1.5 mM to 3 mM will result in 2-4 mutations per the targeted region (29).

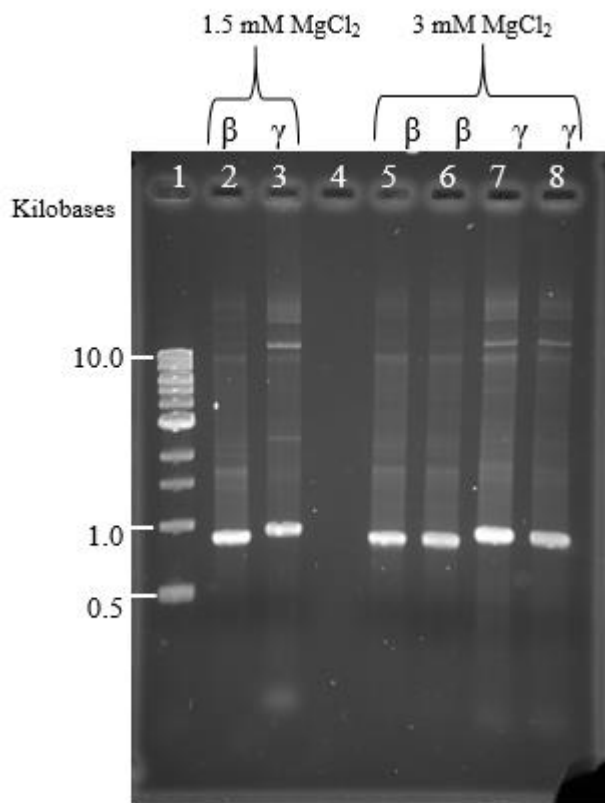


**Figure 5: Horizontal Electrophoresis of epPCR reactions of pESC-LEU  $\beta$ -ENaC and pESC-LEU  $\gamma$ -ENaC.** PCR reactions were analyzed on a 1 % TAE agarose gel at 100V for 1hr. Lane 1, 1kb DNA ladder. Lane 2, pESC-LEU  $\beta$ -ENaC template for PCR reaction with 1.5 mM MgCl<sub>2</sub>. Lane 3, pESC- for PCR reaction with 1.5 mM MgCl<sub>2</sub>. Lane 4, Water. Lane 5 and 6, pESC-LEU  $\beta$ -ENaC template for PCR reaction with 3 mM MgCl<sub>2</sub>. Lane 7 and 8, pESC-LEU  $\gamma$ -ENaC template for PCR reaction with 3 mM MgCl<sub>2</sub>. The gel was stained with 0.25 mg/mL EtBr.

PCR reactions of SCNN1B and SCNN1G with both 1.5 mM and 3 mM MgCl<sub>2</sub> were executed under the same conditions, 94°C for 1 minute, 60-55° C for 1 minute, 72°C for 1 minute, for 25 cycles in a thermocycler. PCR products of the extracellular loop of the  $\beta$ -ENaC gene should result in an 800-870 bp fragment. Analysis of the PCR product by horizontal gel electrophoresis showed that the  $\beta$ -ENaC extracellular loop was successfully amplified (Fig 5, Lanes 1, 5, and 6). The PCR reactions were performed

with 1.5 mM (Fig 5, lanes 2-3) or 3 mM MgCl<sub>2</sub> (Fig 5, lanes 5-8). Both concentrations of MgCl<sub>2</sub> have been shown to promote mutations after amplification (29). The higher the concentration resulted in an increase in nucleotide mutations in the sequence (29). The reactions containing higher concentrations of MgCl<sub>2</sub> (i.e. 3 mM, Fig 5, lanes 5-6) were used in subsequent studies. Mutated regions of the extracellular loop for SCNN1G were saved for future analysis (Fig 5, lanes 2, 7-8).

PCR product was purified using the DNA Clean & Concentrator protocol.

Quantitative analysis of the purified PCR produced was 46.7 ng/μL.

### **Recombination of PCR product and expression vector**

To study mutations on the extracellular loop of βENaC a mutational library was created from the recombination of a digested vector and mutated extracellular loop. For this study the plasmid used was pESC-LEU βγENaC WT (Fig 6). To prepare the expression vector to carry the mutated extracellular loop region for β-ENaC, pESC-LEU β/γ WT was digested with endonucleases (Figure 7). The endonucleases (SexAI and ZraI) used each cut the expression vector at a unique site (Table 2). The WT plasmid was digested in the SCNN1B site to remove a section of the WT extracellular loop (704-1028) for the βENaC subunit. Yeast contains *in vivo* recombination pathways which will be used to recombine a digested vector and the epPCR products. Theoretically, the transformation of both products will result in a mutational library for study (Fig 7). Upon transformation into yeast, the removed extracellular loop region would be replaced with the mutated region made in the epPCR amplification (Fig 7).

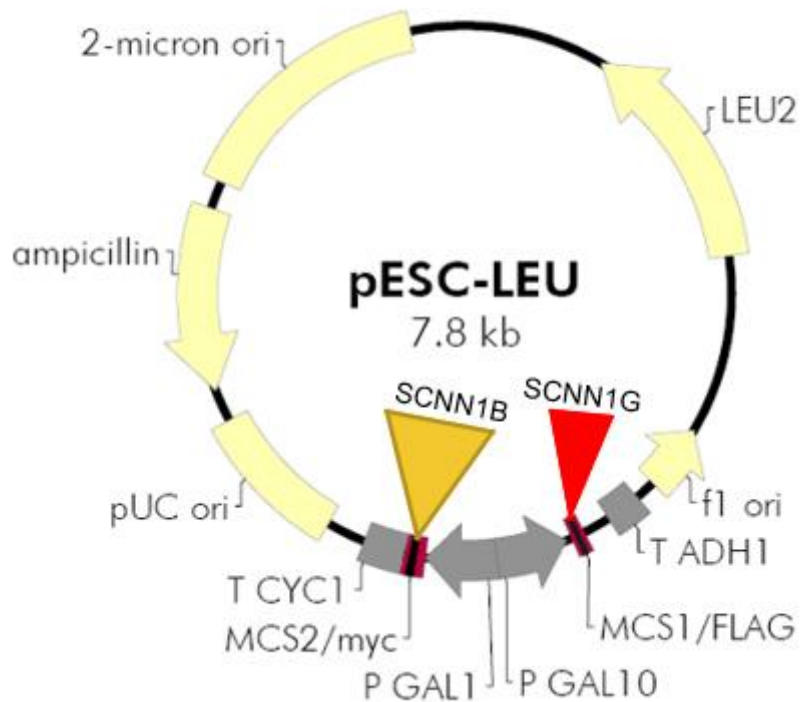


**Figure 6: Schematic of pESC-LEU expression vector.** This is a schematic of the pESC-LEU vector used in this study. The SCNN1B (beta ENaC) and SCNN1G (gamma ENaC) were both cloned previously into this vector. SCNN1G was cloned into the multiple cloning site one. SCNN1B was cloned in the multiple cloning site two. SCNN1B will have a myc epitope sequence and SCNN1G will have a FLAG epitope sequence. This plasmid has growth markers for both *E. coli* (ampicillin resistance) and yeast (LEU 2). The galactose promoters (P GAL1/10) will be used in the expression of this vector. (27)

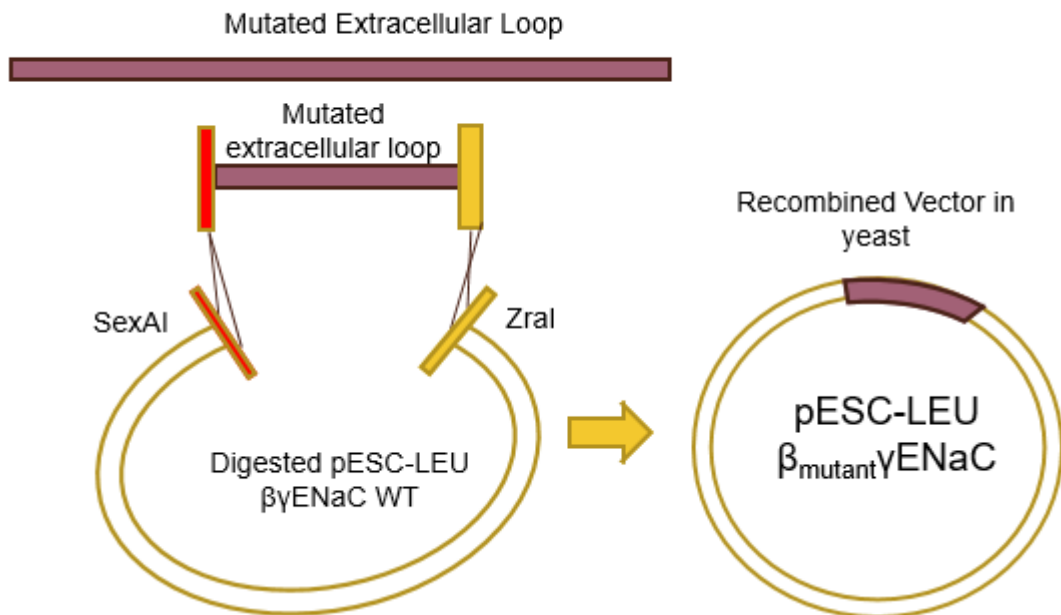


**Fig 7: Schematic depiction of recombination of pESC-LEU  $\beta/\gamma$  ENaC with mutated region.** This diagram is showing the process of creating the mutant plasmid. The PCR product for the extracellular loop of  $\beta$ ENaC and the digested vector will be recombined when transformed into yeast. This will result in a mutational library with each colony containing a different mutant vector.

Two colonies of transformed pESC-LEU  $\beta/\gamma$  WT in ER 2925 cells were isolated and digested with SexAI and ZraI (Fig 8, Table 6). Plasmid samples A (Fig 7, lanes 2-5) and B (Fig 8, lanes 6-9) of pESC-LEU $\beta/\gamma$  WT ENaC were digested at 37°C for one hour and analyzed on 1%TAE agarose gel at 100V. Uncut pESC-LEU  $\beta/\gamma$  WT was analyzed alongside the digested plasmid as a control (Fig 8, lanes 2 and 6). Due to the original size of pESC-LEU (7.8 kb) and the additional input of two cloned ENaC genes (~4 kb), the pESC-LEU  $\beta/\gamma$  ENaC vector should migrate with 12 kb standard. Different structural states of plasmid (i.e. supercoiled, circular) can result in multiple bands (Fig 8, lanes 2 and 6) and when cut will result in a single linear form (Fig 8, lanes 3-4 and 7-8). A shift in fragment size after digestion with two endonucleases means a region was cut out (Fig 8, lanes 5 and 9). The smaller fragment (~300 bp) is not seen in the double digestion

reactions (Fig 7, lanes 5 and 9). Smaller fragments do not stain as easily. To verify the presence of two fragments after double digested of pESC-LEU  $\beta\gamma$  ENaC WT double digestion samples (Fig 8, lanes 5 and 9) were analyzed on a horizontal gel electrophoresis at a lower voltage (Fig 9).

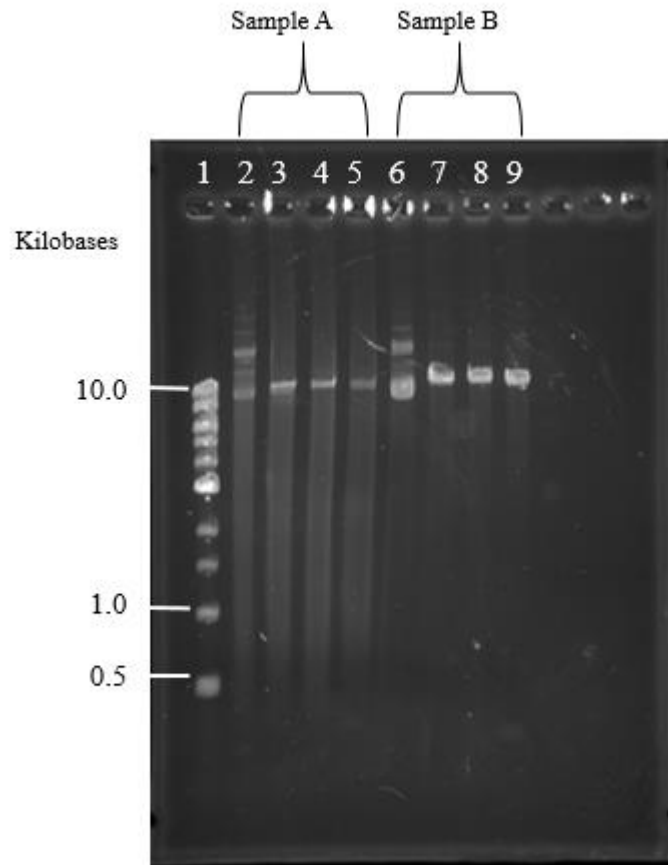


**Figure 8: Horizontal Electrophoresis of Digestion of pESC-LEU  $\beta\gamma$  ENaC.**

Undigested and digested plasmid samples were loaded on a 1 % TAE agarose gel and analyzed at 110V for 1 hour. Lane 1, 1kb DNA Ladder. Lane 2, uncut pESC-LEU  $\beta\gamma$  ENaC from sample A. Lane 3, Digested pESC-LEU  $\beta\gamma$  ENaC from sample A with ZraI. Lane 4, Digested pESC-LEU  $\beta\gamma$  ENaC from sample A with SexAI. Lane 5, Double digestion of pESC-LEU  $\beta\gamma$  ENaC from sample A with ZraI and SexAI. Lane 6, uncut pESC-LEU  $\beta\gamma$  ENaC from sample B. Lane 7, Digested pESC-LEU  $\beta\gamma$  ENaC from sample B with ZraI. Lane 8, Digested pESC-LEU  $\beta\gamma$  ENaC from sample B with SexAI. Lane 9, Double digestion of pESC-LEU  $\beta\gamma$  ENaC from sample B with ZraI and SexAI. The gel was stained with 0.25 mg/mL EtBr.

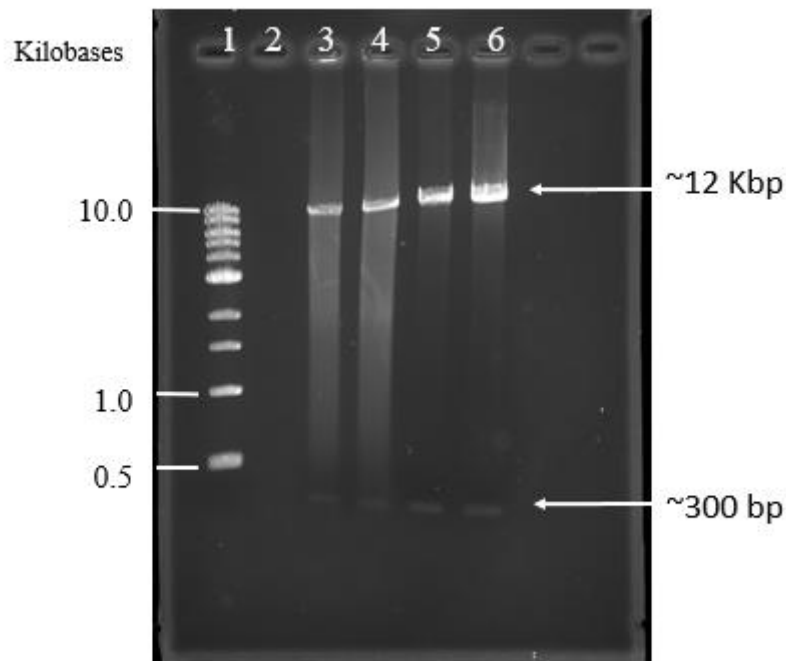


**Figure 9: Digestion of pESC-LEU  $\beta\gamma$  ENaC with ZraI and SexAI.** Digested samples were analyzed on a 1 %TAE agarose gel at 100V for 1 hour. Lane 1, 1kb DNA ladder. Lane 2, empty. Lane 3-4, Double digestion of pESC-LEU  $\beta\gamma$  ENaC from Sample A with ZraI and SexAI. Lane 5-6, Double digestion of pESC-LEU  $\beta\gamma$  ENaC from Sample B with ZraI and SexAI. The gel was stained with 0.25 mg/mL EtBr.

In the horizontal gel electrophoresis analysis of the double digestion of pESC-LEU  $\beta\gamma$  ENaC WT both samples had two fragments of DNA (Fig 9, lanes 3-6). The fragment sizes were about ~12 kb and ~300 bp (Fig 9, lanes 3-6). Both digested samples contained background streaking after staining (Fig 9, lanes 3-6). This could be due to possible RNA contamination. After verification of a smaller fragment (~300 bp) the

fragment of interest (~12 kb) was excised from the gel (Fig 10, lanes 3-6). The excised band was cleaned and purified using the gel extraction protocol previously stated.

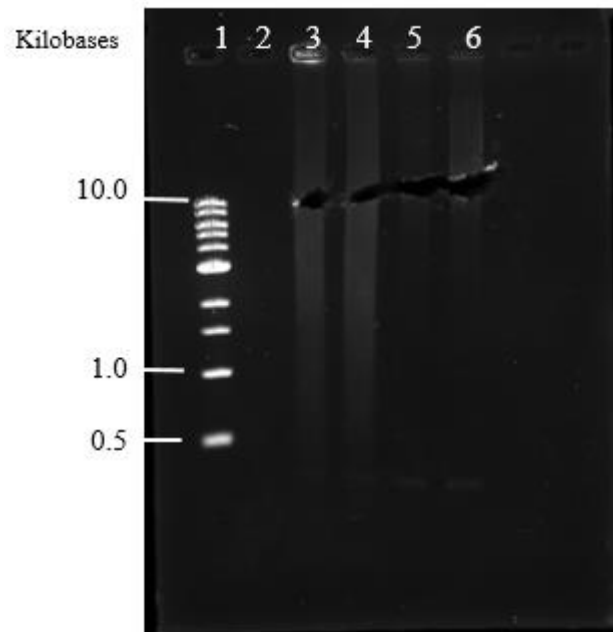


**Figure 10: Gel Extraction of Digested pESC-LEU  $\beta\gamma$  WT.** Fragment of interest (~12kb) was excised. Lane 1, 1kb DNA ladder, Lane 2, empty. Lane 3-4, extracted ~12kb fragment of pESC-LEU  $\beta\gamma$  ENaC from Sample A with ZraI and SexAI. Lane 5-6, extracted ~12kb fragment of digested pESC-LEU  $\beta\gamma$  ENaC from Sample B with ZraI and SexAI. The gel was stained with 0.25 mg/mL EtBr

The purified epPCR product and digested plasmid were both co-transformed into  $\alpha$ -ENaC BY4742 cells for *in vivo* recombination. Yeast cells were plated on selective media for the pESC-LEU and PYES2NTA vector (i.e. glucose-uracil-leucine) for 3-5 days. Yeast cells containing both plasmids took longer to grow. Four colonies were taken at random from the transformation plate and streaked on another plate for continued analysis.

## Qualitative Analysis of ENaC in the Yeast Model System

To further analyze the selected  $\beta$ ENaC mutants in the heterotrimeric complex,  $\alpha\beta\gamma$ ENaC, a qualitative assay was used to look at salt sensitivity as a monitor of ENaC function. This survival dilution assay was used to show the differences in yeast cell growth when  $\alpha\beta\gamma$ ENaC was being expressed compared to that of the mutant- $\alpha\beta\gamma$ ENaC (27). The growth conditions of this assay is the comparison of salt-sensitivity when ENaC is being expressed through a GAL promoters on the pESC-LEU and PYES2NTA expression vectors. Yeast cultures on the glucose-selective media were used as controls (Fig 11, top panel). Additional salt was added to selective media plates to further observe the intensified salt-sensitivity when ENaC was being made. It was expected that when WT ENaC was expressed that the channel would bring in more salt from the media. The purpose of this assay was to observe if there is a difference in salt-sensitivity when ENaC was mutated, specifically in the extracellular loop of the SCNN1B

In the salt- sensitivity assay there was no growth inhibition of any of the yeast samples when grown in glucose (Fig 11, panel A). As expected in 0.5M of NaCl the yeast cells began to exhibit some growth inhibition (Fig 11, panel B), but it was present in all samples. In the yeast cells with just the  $\alpha$ ENaC homotrimeric channel, growth is still not greatly impacted as it is when there is possible formation of the heterotrimeric channel (Fig 11, panels C and D, row 1 and 2). When the  $\alpha\beta\gamma$ ENaC WT sample was in the galactose media there is a large increase of growth inhibition in comparison to the control (Fig 11, panel A and C, row 2). Each yeast sample that contained a mutant complex,  $\alpha\beta_{\text{mutant}}\gamma$ ENaC, the growth was impacted but not as severe when compared to the wildtype  $\alpha\beta\gamma$ . (Fig 11, panel C). In the galactose media with additional salt (0.5 M NaCl)

there was a severe decrease in yeast cell proliferation (Fig 11, D). This has been shown to happen when ENaC expression is turned on yeast cells because of the increase in salt-reabsorption from the media (26-29). The trends of yeast growth were more impacted when ENaC was forming a heterotrimeric channel vs a homotrimeric channel (WT  $\alpha$ ENaC vs WT  $\alpha\beta\gamma$ ENaC). This was expected because prior studies have reported that in nature the heterotrimeric channels is more functional than the homotrimeric channels (6, 8, 11, and 15). In the comparison of the WT  $\alpha\beta\gamma$ ENaC to the  $\alpha\beta_{\text{mutant}}\gamma$ ENaC (Fig 11, panel C and D, rows 3-6) each mutant did not demonstrate the same trend as the wild-type ENaC (Fig 11, panel C and D, row 2). Furthermore, the trend observed indicates  $\alpha\beta_{\text{mutant}}\gamma$ ENaC were not functioning as well as the  $\alpha\beta\gamma$ ENaC. The mutations may be allowing the heterotrimeric complex to be formed but not resulting in ENaC transport to the membrane. Alternatively, difference in functionality may be that residues changed in mutagenesis were critical to either functionality of ENaC, heterotrimeric formation, localization of ENaC to the membrane, or protein stability.



## Confirmation of the Expression of the Beta ENaC Subunit

Confirmation of the expression of the  $\beta$ ENaC subunit was measured through western blot analysis. Yeast cells containing  $\alpha\beta\gamma$ ENaC and  $\alpha\beta_{\text{mutant}}\gamma$ ENaC were lysed after a protein expression protocol and analyzed on a SDS-PAGE gel. The proteins in the gel were transferred to a nitrocellulose membrane and blotted using the Rabbit anti-beta polyclonal antibody (StressMarq Biosciences, Victoria, CA). On the nitrocellulose membrane, there is was a signal for WT  $\beta$ ENaC at  $\sim 70$  kDa (Fig 12, lane 3). In each of the mutant samples there was protein at  $\sim 70$  kDa (Fig 12, lanes 4-7. The proposed size of ENaC is  $\sim 77$  kDa, thus  $\beta$ ENaC were being expressed. Another observation from the immunoblot was the WT  $\alpha\beta\gamma$  ENaC sample has a slightly stronger signal than the mutants (Fig 12, lane 3). It would be interesting to quantitatively measure expression of WT  $\alpha\beta\gamma$  ENaC sample compared to that of the  $\alpha\beta_{\text{mutant}}\gamma$ ENaC samples. Background bands in the samples could be cross-reactivity of the antibody of  $\beta$ ENaC with other products. A way

to test this cross-reactivity is to incubate the membrane with another anti-body for either  $\alpha$ ENaC or  $\gamma$ ENaC.

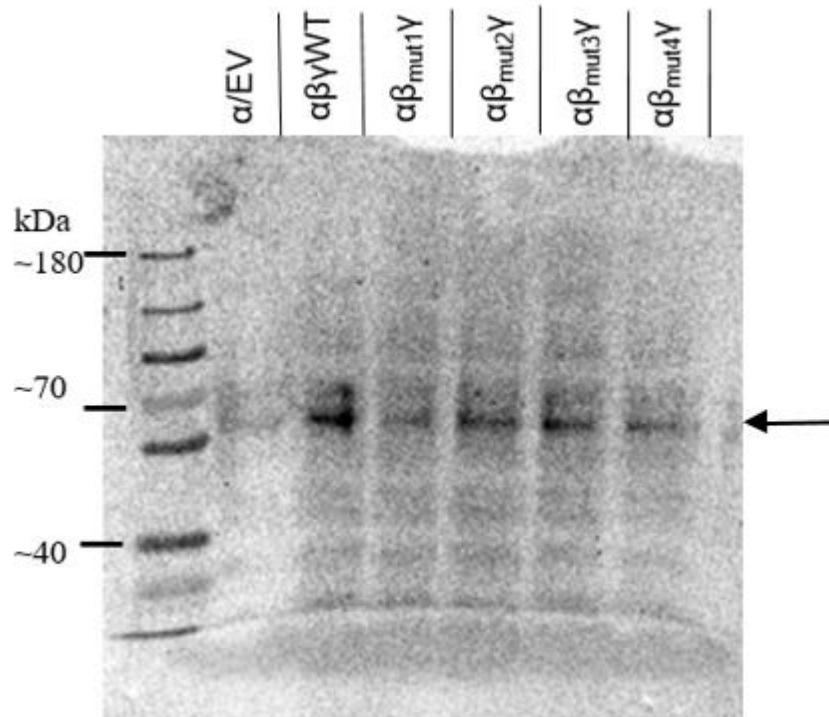


**Figure 12: Immunoblot of  $\beta$ -ENaC mutants using anti-beta antibody.** Loaded 100ng of protein extracted from yeast samples and analyzed on SDS-Page gel. Gel was transferred on a nitrocellulose membrane at 20 V and 1.3 Amps for 20 minutes. Membrane was incubated Rabbit anti-beta polyclonal antibody (StressMarq Biosciences, Victoria, CA). Lane 1, protein ladder. Lane 2, pYES2NTA $\alpha$ /pESC-LEU empty vector protein extract. Lane 3, pYES2NTA $\alpha$ /pESC-LEU WT ENaC protein extract. Lane 4, pYES2NTA $\alpha$ /pESC-LEU $\beta$ mutant1/ $\gamma$  protein extract, Lane 5, pYES2NTA $\alpha$ /pESC-LEU $\beta$ mutant2/ $\gamma$  protein extract. Lane 6, pYES2NTA $\alpha$ /pESC-LEU $\beta$ mutant3/ $\gamma$  ENaC protein extract. Lane 7, pYES2NTA $\alpha$ /pESC-LEU $\beta$ mutant4/ $\gamma$  protein extract. Nitrocellulose membrane was stained using Western Lightning kit.

### Verification of pESC-LEU Expression Vector from Yeast Plasmid Isolation

To prepare for sequence analysis plasmid had to be isolated from yeast. Isolation of yeast plasmid proved very difficult in that the plasmid yield was low and not pure enough for direct sequencing. Isolated yeast plasmids from Beta mutant 1-4 has to be

transformed into Top 10 *E. coli*. This proved beneficial for generating larger DNA concentrations necessary for sequencing. Because the yeast samples contained two expression vectors (i.e. pYES2NTA and pESC-LEU) the isolated plasmids had to be screened to confirm for the pESC-LEU  $\beta\gamma$  ENaC vector. To verify that the plasmid isolated was the pESC-LEU $\beta$ mutant/ $\gamma$  vector(s) each transformed colony was cultured overnight, plasmid was isolated, and digested with XhoI and NheI endonucleases for 1 hour at 37°C. The reason behind changing the endonucleases from ZraI/SexAI to XhoI/NheI was because both enzymes do not cut in the SCNN1B gene. Digestion of pESC-LEU  $\beta/\gamma$  ENaC WT resulted in two fragments of the plasmid (Fig 13, lane 2). Digestion of pYES2NTA  $\alpha$ ENaC WT resulted in three fragments of the plasmid (Fig 13, lane 3). Double digestion reactions were analyzed on a 1 % TAE agarose gel at 100V for 1 hr. If the digested plasmid matches the expected digestion of pESC-LEU  $\beta/\gamma$  ENaC WT (Fig 13, lane 2) then this served as verification that the pESC  $\beta_{\text{mutant}}\gamma$  ENaC plasmid was present in the sample.

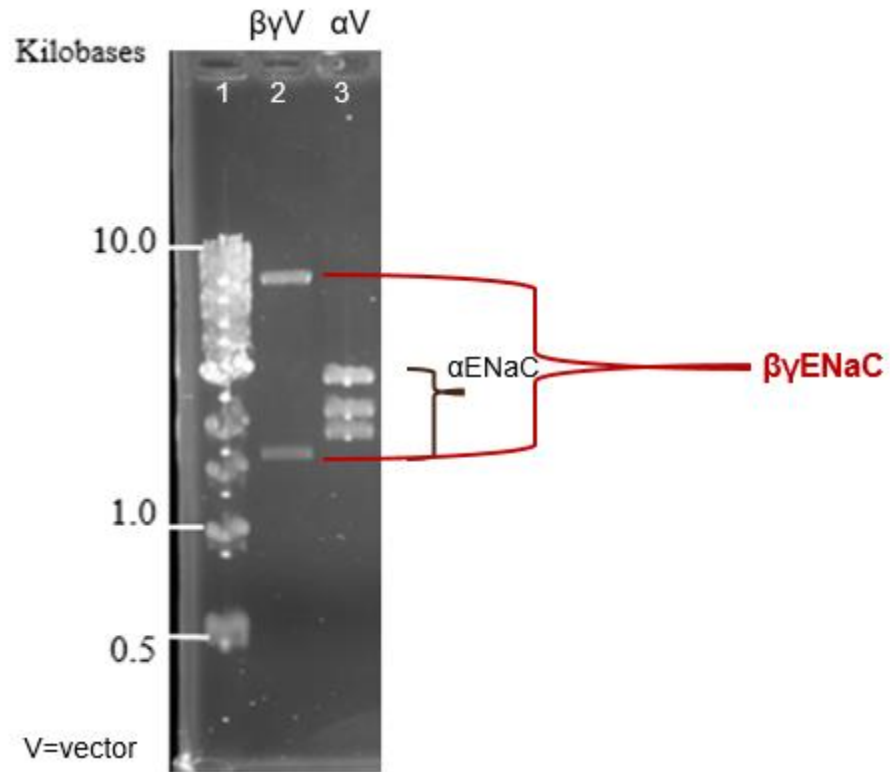


**Figure 13: Digestion of pESC-LEU  $\beta/\gamma$  ENaC WT and pYES2NTA  $\alpha$ ENaC WT.** Both expression vectors were digested with XhoI and NheI at 37° C for 1 hour and analyzed on a 1% TAE agarose gel. Lane 1, 1 kb ladder. Lane 2, digested pESC-LEU  $\beta/\gamma$  ENaC WT. Lane 3, digested pYES2NTA  $\alpha$ ENaC WT.

For Beta mutant 2, three of the samples isolated did not match the WT sample (Fig 14, lanes 3-5) but did match the pYES2NTA  $\alpha$ ENaC plasmid (Fig 13, lane 3). Sample 4 from Beta mutant 2 (Fig 14, lane 6) did match the pESC-LEU  $\beta/\gamma$  ENaC WT digestion (Fig 13, lane 2) and was stored for future analysis. For Beta mutant 3, all of the samples matched the pESC-LEU  $\beta/\gamma$  ENaC WT sample (Fig 15, lanes 3-7). Beta mutant 4 samples were only digested with XhoI (Fig 16, lanes 5, 7, 9, and 10). Sample A from the Beta mutant 4 samples matched DNA migration of the WT uncut pESC-LEU  $\beta/\gamma$  ENaC (Fig 16, lane 5). The remaining samples had lower migrations of DNA matching the ~7.8

kb of pYES2NTA- $\alpha$ ENaC (Fig 16, lanes 9 and 11). Each sample that match pESC-LEU  $\beta\gamma$  ENaC WT digestion (Fig 13, lane 2) was stored for future analysis at  $-20^{\circ}$  C.

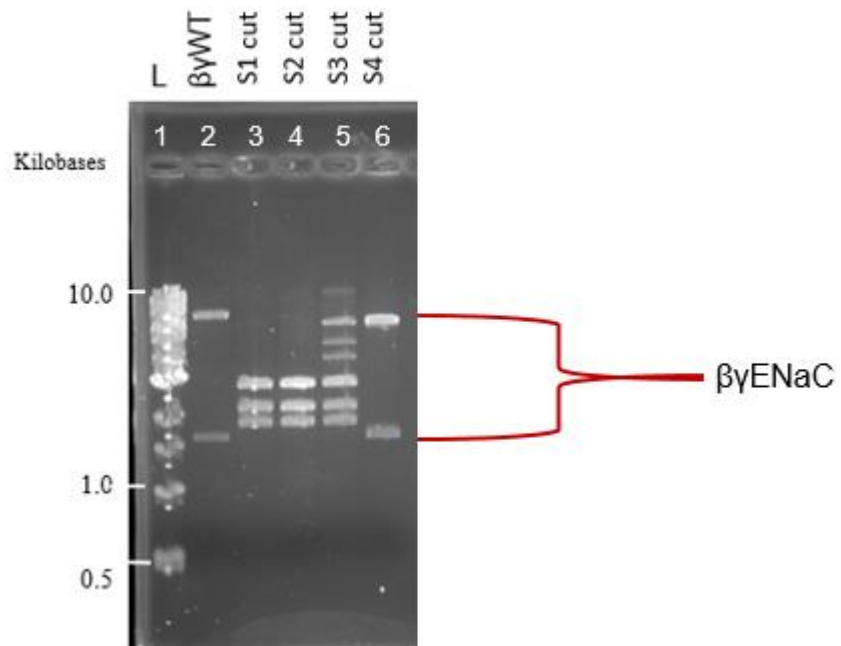


**Figure 14: Double Digestion of Beta mutant 2 samples with XhoI and NheI.** Samples were isolated from transformed Top 10 colonies and digested with endonucleases for 1 hour at  $37^{\circ}$  C. Digested samples were analyzed of a 1% TAE agarose gel for 1 hour at 110V. Lane 1, 1 kb ladder. Lane 2, double digestion of pESC-LEU  $\beta\gamma$  ENaC WT. Lane 3, double digestion of pESC-LEU Beta mutant 2-Sample 1. Lane 4, double digestion of pESC-LEU Beta mutant 2-Sample 2. Lane 5, double digestion of pESC-LEU Beta mutant 2-Sample 3. Lane 6, double digestion of pESC-LEU Beta mutant 2 Sample 4. The gel was stained with 0.25 mg/mL EtBr.

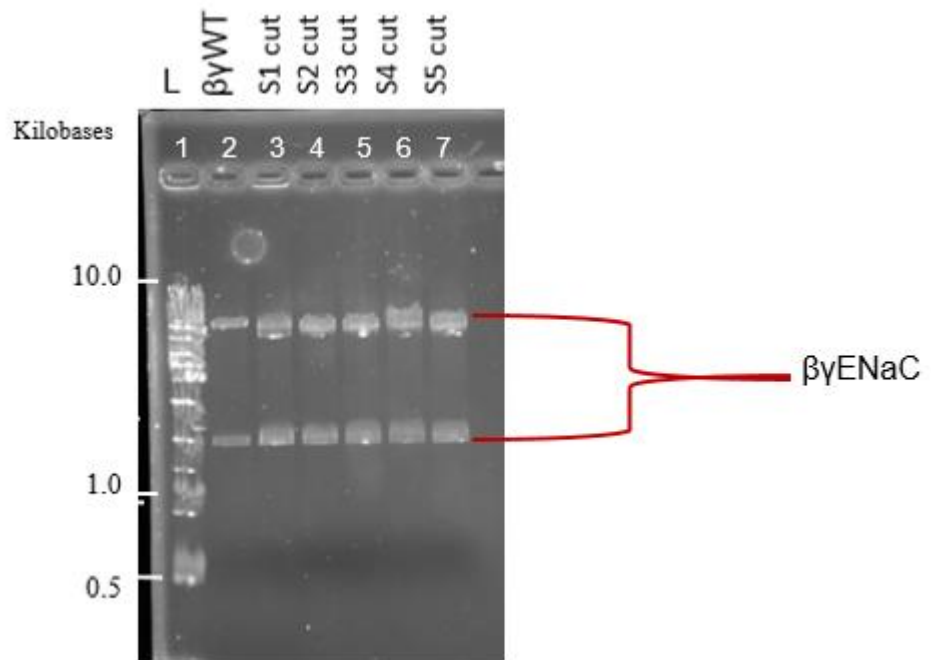


**Figure 15: Double Digestion of Beta mutant 3 samples with XhoI and NheI.** Samples were isolated from transformed Top 10 colonies and digested with endonucleases for 1 hour at 37° C. Digested samples were analyzed of a 1% TAE agarose gel for 1 hour at 110V. Lane 1, 1 kb ladder. Lane 2, double digestion of pESC-LEU  $\beta$ y ENaC WT. Lane 3, double digestion of Beta mutant 3- Sample 1. Lane 4, double digestion of pESC-LEU Beta mutant 3-Sample 2. Lane 5, double digestion of pESC-LEU Beta mutant 3-Sample 3. Lane 6, double digestion of pESC-LEU Beta mutant 3-Sample 4. Lane 7, double digestion of pESC-LEU Beta mutant 3-Sample 5. The gel was stained with 0.25 mg/mL EtBr.

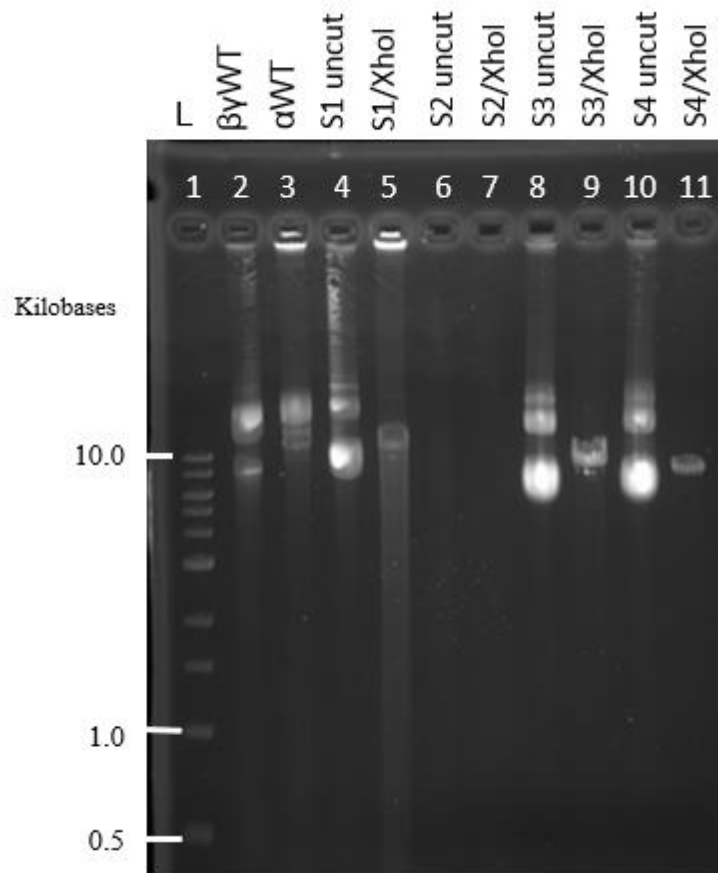


**Figure 16: Single Digestion of Beta mutant 4 samples with XhoI.** Samples were isolated from transformed Top 10 colonies and digested with endonuclease for 1 hour at 37° C. Digested samples were analyzed of a 1% TAE agarose gel for 1 hour and 15 minutes at 100V. Lane 1, 1 kb ladder. Lane 2, uncut pYES2NTA- $\alpha$  ENaC WT. Lane 3, uncut pESC-LEU-  $\beta\gamma$  ENaC WT. Lane 4, uncut Beta mutant 4-sample A. Lane 5, single digested Beta mutant 4-sample A, Lane 6, uncut Beta mutant 4-sample B. Lane 7, single digested Beta mutant 4-sample B. Lane 8, uncut Beta mutant 4-sample C, Lane 9, single digested Beta mutant 4-sample C. Lane 10, uncut Beta mutant 4-sample D, Lane 11, single digested Beta mutant 4-sample D. The gel was stained with 0.25 mg/mL EtBr.

After plasmid isolations of Beta mutant 1 samples efforts to verify the pESC-LEU vector proved difficult (Fig 17). None of the samples matched the pESC-LEU  $\beta\gamma$  ENaC

WT double digestion (Fig 17, lanes 3-7). Each sample (Fig 17, lanes 3-7) revealed contained fragments expected for pYES2NTA- $\alpha$ ENaC digestion (Fig 13, lane 3). The digestion of the plasmids looks to be not fully digested with both enzymes or exhibiting STAR activity. STAR activity is when the selectivity of the endonuclease is changed because of the conditions (i.e. buffer, concentration) of the digestion. In order to isolate the mutant SCNN1B for sequence analysis a high fidelity PCR amplification was used. Using a Phusion polymerase to minimize error rate of amplification the Beta ENaC gene from Beta mutant 1 was amplified using primers that would anneal to SCNN1B (Table 2, Fig 18).

The high fidelity PCR reaction was performed using the high fidelity PCR protocol previously stated. The PCR products were analyzed on a 1% TAE agarose gel for 1 hour at 100V. With a fragment at ~2 kb, the horizontal gel electrophoresis analysis proved that the SCNN1B gene was successfully amplified (Fig 18, lanes 3-4). Lower migration fragment are the oligonucleotide primers. This is known because the control which did not contain a template had this same band (Fig 18, lane 2). To prevent the amplification of annealed primers the concentrations of the primers could be decreased. The PCR product was then cleaned up and stored at -20° C for future analysis.

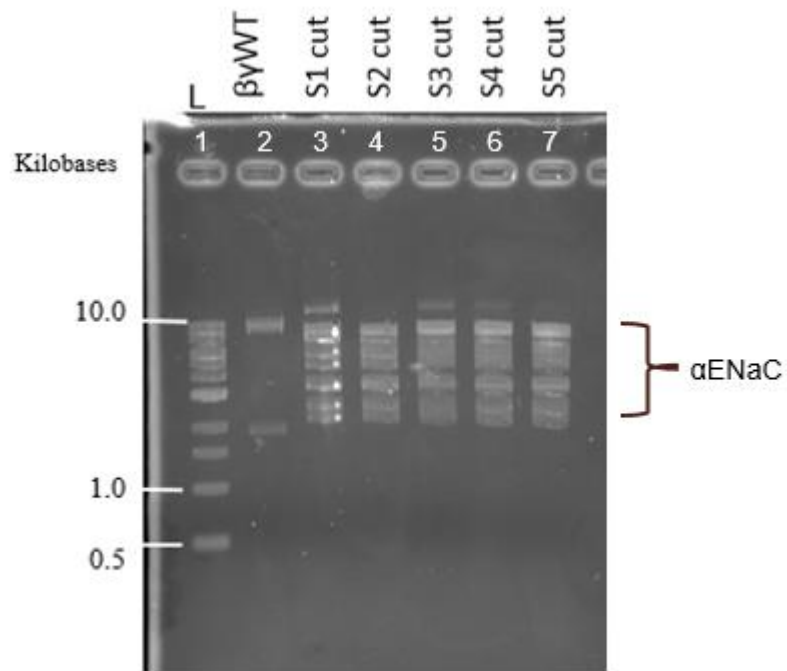


**Figure 17: Double Digestion of Beta mutant 1 samples with XhoI and NheI.** Samples were isolated from transformed Top 10 colonies and digested with endonucleases for 1 hour at 37° C. Digested samples were analyzed of a 1% TAE agarose gel for 1 hour at 110V. Lane 1, 1 kb ladder. Lane 2, double digestion of pESC-LEU βγ ENaC WT. Lane 3, double digestion of Beta mutant 1- Sample 1. Lane 4, double digestion of pESC-LEU Beta mutant 1-Sample 2. Lane 5, double digestion of pESC-LEU Beta mutant 1-Sample 3. Lane 6, double digestion of pESC-LEU Beta mutant 1-Sample 4. Lane 7, double digestion of pESC-LEU Beta mutant 1-Sample 5. The gel was stained with 0.25 mg/mL EtBr.

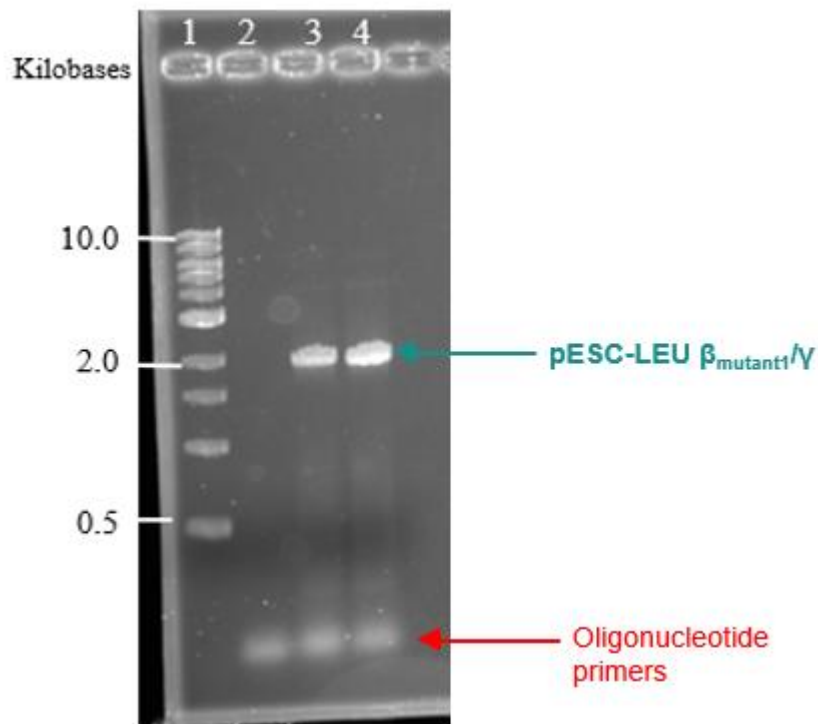


**Figure 18: High Fidelity PCR amplification of SCNN1B in Beta mutant 1 samples.** PCR reaction was prepared using the high fidelity PCR protocol previously stated. PCR product was analyzed on a 1% TAE agarose gel at 100V for 1 hour. Lane 1, 1 kb ladder. Lane 2, PCR mixture with no template. Lane 3, isolated yeast plasmid from Beta mutant 1-sample A with PCR mixture. Lane 4, isolated yeast plasmid from Beta mutant 1-sample B with PCR mixture. The gel was stained with 0.25 mg/mL EtBr.

With the verified plasmids of  $\beta$ ENaC mutants 2-4 and the purified PCR product of  $\beta$ ENaC mutant1 samples were prepared for sequencing using the Quintara Biosciences preparation protocol. Sequence analysis was carried out using four separate primers that would anneal to the SCNN1B region and Gal promoters on the pESC-LEU  $\beta\gamma$  expression vector (Table 3). The primers would result in the sequencing of the entire SCNN1B region. All sequences were aligned using Clustal Omega software. Nucleotide sequences were also translated into amino acid sequences and aligned using the MUSCLE software. Because the SCNN1B gene for Beta mutant 1 had to be amplified it was not possible for

the sequencing of the ends of the gene. This should not affect the results since the region that was sequenced was 1400bp in length and was the region of interest. The remaining samples had the full length gene sequenced.

```
BM1 -----
BM3 ATGCCAGTGAAGAAGTACCTCCTGAAGTGCCTGCACCGGCTGCAGAAGGGCCCAGGCTAC
WT ATGCCAGTGAAGAAGTACCTCCTGAAGTGCCTGCACCGGCTGCAGAAGGGCCCAGGCTAC
BM2 ATGCCAGTGAAGAAGTACCTCCTGAAGTGCCTGCACCGGCTGCAGAAGGGCCCAGGCTAC
BM4 ATGCCAGTGAAGAAGTACCTCCTGAAGTGCCTGCACCGGCTGCAGAAGGGCCCAGGCTAC
```

```
BM1 -----
BM3 ACCTACAAGGAGCTGCTAGTGTGGTACTGCAATAACACCAACACCCACGGCCCC-AAACC
WT ACCTACAAGGAGCTGCTAGTGTGGTACTGCAATAACACCAACACCCACGGCCCCAAACGC
BM2 ACCTACAAGGAGCTGCTAGTGTGGTACTGCAATAACACCAACACCCACGGCCCCAAACGC
BM4 ACCTACAAGGAGCTGCTAGTGTGGTACTGCAATAACACCAACACCCACGGCCCCAAACGC
```

```
BM1 -----
BM3 ATCATCTGTGAGGGGCCAAGAAGAAGGCCATGTGGTTCCTGCTTACGCTGCTCTTCGCC
WT ATCATCTGTGAGGGGCCAAGAAGAAGGCCATGTGGTTCCTGCTTACGCTGCTCTTCGCC
BM2 ATCATCTGTGAGGGGCCAAGAAGAAGGCCATGTGGTTCCTGCTTACGCTGCTCTTCGCC
BM4 ATCATCTGTGAGGGGCCAAGAAGAAGGCCATGTGGTTCCTGCTTACGCTGCTCTTCGCC
*****
```

```
BM1 TGCCCTGGTGTGCTGGCAGTG GGGAGTCTTCATCCA AACCTACCT TAACTGGGAGGTCAG
BM3 TGCCCTGGTGTGCTGGCAGTG GGGAGTCTTCATCCAGACCTACCTGAGCTGGGAGGTCAG
WT TGCCCTGGTGTGCTGGCAGTG GGGAGTCTTCATCCAGACCTACCTGAGCTGGGAGGTCAG
BM2 TGCCCTGGTGTGCTGGCAGTG GGGAGTCTTCATCCAGACCTACCTGAGCTGGGAGGTCAG
BM4 TGCCCTGGTGTGCTGGCAGTG GGGAGTCTTCATCCAGACCTACCTGAGCTGGGAGGTCAG
***** * *****
```

```
BM1 CGTCTCGCTCTCCATGGGCTTCAAGACGATGAAC TCCCGCGGT CACCGTCTGCAATTC
BM3 CGTCTCGCTCTC ATGGGCTTCAAGACGATGAAC TCCCGCGGT CACCGTCTGCAATTC
WT CGTCTCGCTCTCCATGGGCTTCAAGACGATGAAC TCCCGCGGT CACCGTCTGCAATTC
BM2 CGTCTCGCTCTCCATGGGCTTCAAGACGATGAAC TCCCGCGGT CACCGTCTGCAATTC
BM4 CGTCTCGCTCTCCATGGGCTTCAAGACGATGAAC TCCCGCGGT CACCGTCTGCAATTC
*****
```

```
BM1 CAGCCCTTCCAGTACTCCAAGGTCA GCACTTGCTCAAGGACTTGGATGAGCTAATGGA
BM3 CAGCCCTTCCAGTACTCCAAGGTCA GCACTTGCTCAAGGACTTGGATGAGCTAATGGA
WT CAGCCCTTCCAGTACTCCAAGGTCA GCACTTGCTCAAGGACTTGGATGAGCTAATGGA
BM2 CAGCCCTTCCAGTACTCCAAGGTCA GCACTTGCTCAAGGACTTGGATGAGCTAATGGA
BM4 CAGCCCTTCCAGTACTCCAAGGTCA GCACTTGCTCAAGGACTTGGATGAGCTAATGGA
*****
```

```
BM1 GGCAGTCCTGGAAAAGATTCTGGCTCCAGAGGCCAGCCACAGCAACACCACCAGGACCCT
BM3 GGCAGTCCTGGAAAAGATTCTGGCTCCAGAGGCCAGCCACAGCAACACCACCAGGACCCT
WT GGCAGTCCTGGAAAAGATTCTGGCTCCAGAGGCCAGCCACAGCAACACCACCAGGACCCT
BM2 GGCAGTCCTGGAAAAGATTCTGGCTCCAGAGGCCAGCCACAGCAACACCACCAGGACCCT
BM4 GGCAGTCCTGGAAAAGATTCTGGCTCCAGAGGCCAGCCACAGCAACACCACCAGGACCCT
*****
```

```
BM1 GAACTTTACCATCTGGAACCACACACCCTGGTCCTTATTGATGAGCGGAACCCCTGACCA
BM3 GAACTTTACCATCTGGAACCACACACCCTGGTCCTTATTGATGAGCGGAACCCCTGACCA
WT GAACTTTACCATCTGGAACCACACACCCTGGTCCTTATTGATGAGCGGAACCCCTGACCA
BM2 GAACTTTACCATCTGGAACCACACACCCTGGTCCTTATTGATGAGCGGAACCCCTGACCA
BM4 GAACTTTACCATCTGGAACCACACACCCTGGTCCTTATTGATGAGCGGAACCCCTGACCA
```

```

*****
BM1      CCCGGTGGTTCTCAATTTGTTTGGGGACAGTTCACAACAGCAGCAACCCGGCTCCAGGAAG
BM3      CCCGGTGGTTCTCAATTTGTTTGGGGACAGTTCACAACAGCAGCAACCCGGCTCCAGGAAG
WT       CCCGGTGGTTCTCAATTTGTTTGGGGACAGCCACAACAGCAGCAACCCGGCTCCAGGAAG
BM2      CCCGGTGGTTCTCAATTTGTTTGGGGACAGTTCACAACAGCAGCAACCCGGCTCCAGGAAG
BM4      CCCGGTGGTTCTCAATTTGTTTGGGGACAGTTCACAACAGCAGCAACCCGGCTCCAGGAAG
*****

BM1      CACCTGCAATGCCCAGGGATGCAAAGTGGCCATGAGGCTGTGCAGTGCCAATGGAAGTGT
BM3      CACCTGCAATGCCCAGGGATGCAAAGTGGCCATGAGGCTGTGCAGTGCCAATGGAAGTGT
WT       CACCTGCAATGCCCAGGGATGCAAAGTGGCCATGAGGCTGTGCAGTGCCAATGGAAGTGT
BM2      CACCTGCAATGCCCAGGGATGCAAAGTGGCCATGAGGCTGTGCAGTGCCAATGGAAGTGT
BM4      CACCTGCAATGCCCAGGGATGCAAAGTGGCCATGAGGCTGTGCAGTGCCAATGGAAGTGT
*****

BM1      GTGTACCTTGCGGAACCTTACCAGTGCCACCCAGGCCGTAAGTGTGGTACATCCTGCA
BM3      GTGTACCTTGCGGAACCTTACCAGTGCCACCCAGGCCGTAAGTGTGGTACATCCTGCA
WT       GTGTACCTTGCGGAACCTTACCAGTGCCACCCAGGCCGTAAGTGTGGTACATCCTGCA
BM2      GTGTACCTTGCGGAACCTTACCAGTGCCACCCAGGCCGTAAGTGTGGTACATCCTGCA
BM4      GTGTACCTTGCGGAACCTTACCAGTGCCACCCAGGCCGTAAGTGTGGTACATCCTGCA
*****

BM1      GGCCACCAACATCTTCTCACAAGTGCTTCCTCAGGACCTGGTGGGGATGGGCTATGCCCC
BM3      GGCCACCAACATCTTCTCACAAGTGCTTCCTCAGGACCTGGTGGGGATGGGCTATGCCCC
WT       GGCCACCAACATCTTCTCACAAGTGCTTCCTCAGGACCTGGTGGGGATGGGCTATGCCCC
BM2      GGCCACCAACATCTTCTCACAAGTGCTTCCTCAGGACCTGGTGGGGATGGGCTATGCCCC
BM4      GGCCACCAACATCTTCTCACAAGTGCTTCCTCAGGACCTGGTGGGGATGGGCTATGCCCC
*****

BM1      TGATCGCATAATCCTAGCTTGCCTGTTTGGAACAGAGCCCTGCAGTCATCGGAACCTCAC
BM3      TGATCGCATAATCCTAGCTTGCCTGTTTGGAACAGAGCCCTGCAGTCATCGGAACCTCAC
WT       TGATCGCATAATCCTAGCTTGCCTGTTTGGAACAGAGCCCTGCAGTCATCGGAACCTCAC
BM2      TGATCGCATAATCCTAGCTTGCCTGTTTGGAACAGAGCCCTGCAGTCATCGGAACCTCAC
BM4      TGATCGCATAATCCTAGCTTGCCTGTTTGGAACAGAGCCCTGCAGTCATCGGAACCTCAC
*****

BM1      GCCTATCTTCTACCCTGATTATGGCAACTGCTACATCTTCAACTGGGGCATGACAGAGGA
BM3      GCCTATCTTCTACCCTGATTATGGCAACTGCTACATCTTCAACTGGGGCATGACAGAGGA
WT       GCCTATCTTCTACCCTGATTATGGCAACTGCTACATCTTCAACTGGGGCATGACAGAGGA
BM2      GCCTATCTTCTACCCTGATTATGGCAACTGCTACATCTTCAACTGGGGCATGACAGAGGA
BM4      GCCTATCTTCTACCCTGATTATGGCAACTGCTACATCTTCAACTGGGGCATGACAGAGGA
*****

BM1      GACACTTCCTTCTGCCAACCCCTGGGACTGAATTTGGTCTCAAGTTGATCCTGGACATCGG
BM3      GACACTTCCTTCTGCCAACCCCTGGGACTGAATTTGGTCTCAAGTTGATCCTGGACATCGG
WT       GACACTTCCTTCTGCCAACCCCTGGGACTGAATTTGGTCTCAAGTTGATCCTGGACATCGG
BM2      GACACTTCCTTCTGCCAACCCCTGGGACTGAATTTGGTCTCAAGTTGATCCTGGACATCGG
BM4      GACACTTCCTTCTGCCAACCCCTGGGACTGAATTTGGTCTCAAGTTGATCCTGGACATCGG
*****

BM1      TCAGGAGGACTATGTCCCCTTCCTTGCGTCCACAGCAGGGGCTAGGCTGATGCTTCATGA
BM3      TCAGGAGGACTATGTCCCCTTCCTTGCGTCCACAGCAGGGGCTAGGCTGATGCTTCATGA
WT       TCAGGAGGACTATGTCCCCTTCCTTGCGTCCACAGCAGGGGCTAGGCTGATGCTTCATGA
BM2      TCAGGAGGACTATGTCCCCTTCCTTGCGTCCACAGCAGGGGCTAGGCTGATGCTTCATGA
BM4      TCAGGAGGACTATGTCCCCTTCCTTGCGTCCACAGCAGGGGCTAGGCTGATGCTTCATGA
*****

```

BM1 GCAGAGGACGTACCCCTTCATTAGAGAGGAGGGCATCTATGCCATGGCAGGAACCTGAGAC  
BM3 GCAGAGGACGTACCCCTTCATTAGAGAGGAGGGCATCTATGCCATGGCAGGAACCTGAGAC  
WT GCAGAGGACGTACCCCTTCATTAGAGAGGAGGGCATCTATGCCATGGCAGGAACCTGAGAC  
BM2 GCAGAGGACGTACCCCTTCATTAGAGAGGAGGGCATCTATGCCATGGCAGGAACCTGAGAC  
BM4 GCAGAGGACGTACCCCTTCATTAGAGAGGAGGGCATCTATGCCATGGCAGGAACCTGAGAC  
\*\*\*\*\*

BM1 GTCTATTGGGGTGCTGGTGGACAAGCTGCAACGCAAGGGGGAGCCCTACAGTCCCTGCAC  
BM3 GTCTATTGGGGTGCTGGTGGACAAGCTGCAACGCAAGGGGGAGCCCTACAGTCCCTGCAC  
WT GTCTATTGGGGTGCTGGTGGACAAGCTGCAACGCAAGGGGGAGCCCTACAGTCCCTGCAC  
BM2 GTCTATTGGGGTGCTGGTGGACAAGCTGCAACGCAAGGGGGAGCCCTACAGTCCCTGCAC  
BM4 GTCTATTGGGGTGCTGGTGGACAAGCTGCAACGCAAGGGGGAGCCCTACAGTCCCTGCAC  
\*\*\*\*\*

BM1 CATGAACGGCTCCGATGTTGCCATAAAGAACCTCTACAGTGTCTACAACACCACCTATTC  
BM3 CATGAACGGCTCCGATGTTGCCATAAAGAACCTCTACAGTGTCTACAACACCACCTATTC  
WT CATGAACGGCTCCGATGTTGCCATAAAGAACCTCTACAGTGTCTACAACACCACCTATTC  
BM2 CATGAACGGCTCCGATGTTGCCATAAAGAACCTCTACAGTGTCTACAACACCACCTATTC  
BM4 CATGAACGGCTCCGATGTTGCCATAAAGAACCTCTACAGTGTCTACAACACCACCTATTC  
\*\*\*\*\*

BM1 CATCCAGGCCTGTCTTCATTCCCTGTTTCCAAGACCACATGATCCGTAACCTGCAGTTGTGG  
BM3 CATCCAGGCCTGTCTTCATTCCCTGTTTCCAAGACCACATGATCCGTAACCTGCAGTTGTGG  
WT CATCCAGGCCTGTCTTCATTCCCTGTTTCCAAGACCACATGATCCGTAACCTGCAGTTGTGG  
BM2 CATCCAGGCCTGTCTTCATTCCCTGTTTCCAAGACCACATGATCCGTAACCTGCAGTTGTGG  
BM4 CATCCAGGCCTGTCTTCATTCCCTGTTTCCAAGACCACATGATCCGTAACCTGCAGTTGTGG  
\*\*\*\*\*

BM1 CCACTACTTATACCCACTGCCTGAAGGAGAGAAATACTGCAACAACAGGGACTTCCCAGA  
BM3 CCACTACTTATACCCACTGCCTGAAGGAGAGAAATACTGCAACAACAGGGACTTCCCAGA  
WT CCACTACTTATACCCACTGCCTGAAGGAGAGAAATACTGCAACAACAGGGACTTCCCAGA  
BM2 CCACTACTTATACCCACTGCCTGAAGGAGAGAAATACTGCAACAACAGGGACTTCCCAGA  
BM4 CCACTACTTATACCCACTGCCTGAAGGAGAGAAATACTGCAACAACAGGGACTTCCCAGA  
\*\*\*\*\*

BM1 CTGGGCCTATTGCTATCTAAACCTGCAGATGAGTGTGACCCAGAGAGAGACCTGCCTCAG  
BM3 CTGGGCCTATTGCTATCTAAACCTGCAGATGAGTGTGACCCAGAGAGAGACCTGCCTCAG  
WT CTGGGCCTATTGCTATCTAAACCTGCAGATGAGTGTGACCCAGAGAGAGACCTGCCTCAG  
BM2 CTGGGCCTATTGCTATCTAAACCTGCAGATGAGTGTGACCCAGAGAGAGACCTGCCTCAG  
BM4 CTGGGCCTATTGCTATCTAAACCTGCAGATGAGTGTGACCCAGAGAGAGACCTGCCTCAG  
\*\*\*\*\*

BM1 CATGTGCAAGGAGTCTGCAATGACACCCAGTATAAGATGACCATCTCCATGGCTGACTG  
BM3 CATGTGCAAGGAGTCTGCAATGACACCCAGTATAAGATGACCATCTCCATGGCTGACTG  
WT CATGTGCAAGGAGTCTGCAATGACACCCAGTATAAGATGACCATCTCCATGGCTGACTG  
BM2 CATGTGCAAGGAGTCTGCAATGACACCCAGTATAAGATGACCATCTCCATGGCTGACTG  
BM4 CATGTGCAAGGAGTCTGCAATGACACCCAGTATAAGATGACCATCTCCATGGCTGACTG  
\*\*\*\*\*

BM1 GCCATCTGAGGCCTCTGAGGATTGGATCTTACATGTCTGTCTCAGGAGCGGGACCAGAG  
BM3 GCCATCTGAGGCCTCTGAGGATTGGATCTTACATGTCTGTCTCAGGAGCGGGACCAGAG  
WT GCCATCTGAGGCCTCTGAGGATTGGATCTTACATGTCTGTCTCAGGAGCGGGACCAGAG  
BM2 GCCATCTGAGGCCTCTGAGGATTGGATCTTACATGTCTGTCTCAGGAGCGGGACCAGAG  
BM4 GCCATCTGAGGCCTCTGAGGATTGGATCTTACATGTCTGTCTCAGGAGCGGGACCAGAG  
\*\*\*\*\*

BM1 CTCGAATATCACCCCTGAGCAGGAAGGGTATTGTCAAGCTCAATATCTACTTCCAAGAGTT  
BM3 CTCGAATATCACCCCTGAGCAGGAAGGGTATTGTCAAGCTCAATATCTACTTCCAAGAGTT  
WT CTCGAATATCACCCCTGAGCAGGAAGGGTATTGTCAAGCTCAATATCTACTTCCAAGAGTT  
BM2 CTCGAATATCACCCCTGAGCAGGAAGGGTATTGTCAAGCTCAATATCTACTTCCAAGAGTT  
BM4 CTCGAATATCACCCCTGAGCAGGAAGGGTATTGTCAAGCTCAATATCTACTTCCAAGAGTT  
\*\*\*\*\*

```

BM1      CAACTACCGTACCATTGAGGAATCTCCAGCCAACAATATTGTGTGGCTGCTCTCTAACCT
BM3      CAACTACCGTACCATTGAGGAATCTCCAGCCAACAATATTGTGTGGCTGCTCTCTAACCT
WT       CAACTACCGTACCATTGAGGAATCTCCAGCCAACAATATTGTGTGGCTGCTCTCTAACCT
BM2      CAACTACCGTACCATTGAGGAATCTCCAGCCAACAATATTGTGTGGCTGCTCTCTAACCT
BM4      CAACTACCGTACCATTGAGGAATCTCCAGCCAACAATATTGTGTGGCTGCTCTCTAACCT
*****

BM1      GGGGGGCCA-----
BM3      GGGGGGCCAGTTTGGCTTCTGGATGGGGGGCTCGGTGCTGTGCCTCATTGAGTTTGGGGA
WT       GGGGGGCCAGTTTGGCTTCTGGATGGGGGGCTCGGTGCTGTGCCTCATTGAGTTTGGGGA
BM2      GGGGGGCCAGTTTGGCTTCTGGATGGGGGGCTCGGTGCTGTGCCTCATTGAGTTTGGGGA
BM4      GGGGGGCCAGTTTGGCTTCTGGATGGGGGGCTCGGTGCTGTGCCTCATTGAGTTTGGGGA
*****

```

**Figure 19: Multiple DNA Sequence Alignment of Beta-ENaC.** The nucleotide sequence of the  $\beta$ ENaC mutants were aligned with the SCNN1B nucleotide sequence from *Mus musculus*. Asterisks reveal conserved regions. Dashed lines represent gaps. Sequences highlighted with colors represent mutations in each mutant. Clustal Omega software was used to align the nucleotide sequences.

**Table 5: Characterization of Nucleic Acid Changes in Beta Mutant 1-4**

Sample	Nucleotide Mutant
Beta mutant 1	X201G, G217A, A326G, C510T, T745C
Beta mutant 2	A326G, C510T
Beta mutant 3	C252T, A326G, C510T
Beta mutant 4	A326G, C510T

```

BM1      ----- 0
WT       MPVKKYLKCLHRLQKPGYTYKELLVWYCNNTNTHGPKRIICEGPKKKAMWFLLLFA 60
BM2      MPVKKYLKCLHRLQKPGYTYKELLVWYCNNTNTHGPKRIICEGPKKKAMWFLLLFA 60
BM3      -----MWFLLLFA 10
BM4      MPVKKYLKCLHRLQKPGYTYKELLVWYCNNTNTHGPKRIICEGPKKKAMWFLLLFA 60

BM1      -----MGFKTMNFPVAVTCNSSPFQYSKVRHLLKDLDELME 36
WT       CLVCWQWGVFIQTYLSWEVSVLSMFGFKTMNFPVAVTCNSSPFQYSKVRHLLKDLDELME 120
BM2      CLVCWQWGVFIQTYLSWEVSVLSMFGFKTMNFPVAVTCNSSPFQYSKVRHLLKDLDELME 120
BM3      CLVCWQWGVFIQTYLSWEVSVLSMFGFKTMNFPVAVTCNSSPFQYSKVRHLLKDLDELME 70
BM4      CLVCWQWGVFIQTYLSWEVSVLSMFGFKTMNFPVAVTCNSSPFQYSKVRHLLKDLDELME 120
*****:*****

BM1      AVLEKILAPEASHSNTTRTLNFTIWNHTPLVLIDERNPDHPVVLNLFGDSHNSSNPAPGS 96
WT       AVLEKILAPEASHSNTTRTLNFTIWNHTPLVLIDERNPDHPVVLNLFGDSHNSSNPAPGS 180
BM2      AVLEKILAPEASHSNTTRTLNFTIWNHTPLVLIDERNPDHPVVLNLFGDSHNSSNPAPGS 180
BM3      AVLEKILAPEASHSNTTRTLNFTIWNHTPLVLIDERNPDHPVVLNLFGDSHNSSNPAPGS 130
BM4      AVLEKILAPEASHSNTTRTLNFTIWNHTPLVLIDERNPDHPVVLNLFGDSHNSSNPAPGS 180
*****

BM1      TCNAQGCKVAMRLCSANGTVCTLRNFTSATQAVTEWYILQATNIFSQVLPQDLVGMGYAP 156
WT       TCNAQGCKVAMRLCSANGTVCTLRNFTSATQAVTEWYILQATNIFSQVLPQDLVGMGYAP 240
BM2      TCNAQGCKVAMRLCSANGTVCTLRNFTSATQAVTEWYILQATNIFSQVLPQDLVGMGYAP 240
BM3      TCNAQGCKVAMRLCSANGTVCTLRNFTSATQAVTEWYILQATNIFSQVLPQDLVGMGYAP 190
BM4      TCNAQGCKVAMRLCSANGTVCTLRNFTSATQAVTEWYILQATNIFSQVLPQDLVGMGYAP 240
*****

```

BM1	DRIILACL <b>I</b> GTTEPCSHRNFTPIFYPDYGNICYIFNWGMTEETLPSANPGTEFGLKLILDIG	216
WT	DRIILACLFGTEPCSHRNFTPIFYPDYGNICYIFNWGMTEETLPSANPGTEFGLKLILDIG	300
BM2	DRIILACLFGTEPCSHRNFTPIFYPDYGNICYIFNWGMTEETLPSANPGTEFGLKLILDIG	300
BM3	DRIILACLFGTEPCSHRNFTPIFYPDYGNICYIFNWGMTEETLPSANPGTEFGLKLILDIG	250
BM4	DRIILACLFGTEPCSHRNFTPIFYPDYGNICYIFNWGMTEETLPSANPGTEFGLKLILDIG	300
	*****.*****	
BM1	QEDYVPFLASTAGARLML <b>R</b> EQRTYPFIREEGIYAMAGTETSIGVLVDKLQRKGEPEYSPCT	276
WT	QEDYVPFLASTAGARLMLHEQRTYPFIREEGIYAMAGTETSIGVLVDKLQRKGEPEYSPCT	360
BM2	QEDYVPFLASTAGARLMLHEQRTYPFIREEGIYAMAGTETSIGVLVDKLQRKGEPEYSPCT	360
BM3	QEDYVPFLASTAGARLMLHEQRTYPFIREEGIYAMAGTETSIGVLVDKLQRKGEPEYSPCT	310
BM4	QEDYVPFLASTAGARLMLHEQRTYPFIREEGIYAMAGTETSIGVLVDKLQRKGEPEYSPCT	360
	*****.*****	
BM1	MNGSDVAIKNLYSVYNTTYSIQACLHSCFQDHMIRNCSCGHYLYPLPEGEKYCNRDFPD	336
WT	MNGSDVAIKNLYSVYNTTYSIQACLHSCFQDHMIRNCSCGHYLYPLPEGEKYCNRDFPD	420
BM2	MNGSDVAIKNLYSVYNTTYSIQACLHSCFQDHMIRNCSCGHYLYPLPEGEKYCNRDFPD	420
BM3	MNGSDVAIKNLYSVYNTTYSIQACLHSCFQDHMIRNCSCGHYLYPLPEGEKYCNRDFPD	370
BM4	MNGSDVAIKNLYSVYNTTYSIQACLHSCFQDHMIRNCSCGHYLYPLPEGEKYCNRDFPD	420
	*****	
BM1	WAYCYLNLQMSVTQRETCLSMCKESCNDTQYKMTISMADWPSEASEDWILHVLSQERDQS	396
WT	WAYCYLNLQMSVTQRETCLSMCKESCNDTQYKMTISMADWPSEASEDWILHVLSQERDQS	480
BM2	WAYCYLNLQMSVTQRETCLSMCKESCNDTQYKMTISMADWPSEASEDWILHVLSQERDQS	480
BM3	WAYCYLNLQMSVTQRETCLSMCKESCNDTQYKMTISMADWPSEASEDWILHVLSQERDQS	430
BM4	WAYCYLNLQMSVTQRETCLSMCKESCNDTQYKMTISMADWPSEASEDWILHVLSQERDQS	480
	*****	
BM1	SNITLSRKGIVKLNLYFQEFNYRTIEESPANNIVWLLSNLGG-----	438
WT	SNITLSRKGIVKLNLYFQEFNYRTIEESPANNIVWLLSNLGGQFGFWMGGSVLCLIEFGE	540
BM2	SNITLSRKGIVKLNLYFQEFNYRTIEESPANNIVWLLSNLGGQFGFWMGGSVLCLIEFGE	540
BM3	SNITLSRKGIVKLNLYFQEFNYRTIEESPANNIVWLLSNLGGQFGFWMGGSVLCLIEFGE	490
BM4	SNITLSRKGIVKLNLYFQEFNYRTIEESPANNIVWLLSNLGGQFGFWMGGSVLCLIEFGE	540
	*****	
BM1	-----	438
WT	I I I D F I W I T I I K L V A S C K G L R R R R P Q A P Y T G P P P T V A E L V E A H T N F G F Q P D T T S C R P H G E	600
BM2	I I I D F I W I T I I K L V A S C K G L R R R R P Q A P Y T G P P P T V A E L V E A H T N F G F Q P D T T S C R P H G E	600
BM3	I I I D F I W I T I I K L V A S C K G L R R R R P Q A P Y T G P P P T V A E L V E A H T N F G F Q P D T T S C R P H G E	550
BM4	I I I D F I W I T I I K L V A S C K G L R R R R P Q A P Y T G P P P T V A E L V E A H T N F G F Q P D T T S C R P H G E	600
BM1	-----	438
WT	VYPDQQTLPIPGTPPPNYDSLRLQPLDTMESDSEVEAI	638
BM2	VYPDQQTLPIPGTPPPNYDSLRLQPLDTMESDSEVEAI	638
BM3	VYPDQQTLPIPGTPPPNYDSLRLQPLDTMESDSEVEAI	588
BM4	VYPDQQTLPIPGTPPPNYDSLRLQPLDTMESDSEVEAI	638

**Figure 20: Multiple Amino Acid Sequence Alignment of Beta-ENaC.** The amino acid sequence of the  $\beta$ ENaC mutants were aligned with the  $\beta$ ENaC amino acid sequence from *Mus musculus*. Asterisks reveal conserved regions. Dashed lines represent gaps. A semi-colon represents a mutation with high similarity. A period represents a mutation with weak similarity. Changes highlighted in yellow are not conserved amongst the samples. Nucleotide sequences were translated into amino acid sequences using ExPasy and aligned with MUSCLE software.

**Table 6: Characterization of Amino Acid Changes in Beta Mutant 1**

Beta Mutant 1	
F165L: Phenylalanine to Leucine	Possible structural change of complex
H235R: Histidine to Arginine	Possible changes in structure and/or non-covalent interactions

According to the sequencing information only one of the samples, Beta mutant 1, resulted in enough nucleotide changes for codon mutations (Fig 18, Table 6). Beta mutant 1 had two mutations and that was F165L and H235R (Table 6). Both phenylalanine and leucine amino acids are classified as hydrophobic residues. The biggest difference between the residues is their size. Phenylalanine had a large aromatic structure on its side chain. This loss of aromatic side chain could reduce rigidity at that location. This loss of structural rigidity could reorient the extracellular loop interaction with other residues on the loop of interacting subunits. The second mutation was a histidine to arginine mutation (Table 6). Arginine and histidine both are basic amino acids. Histidine has a pKa closer to physiological pH so it is able to either accept or donate protons. The change to an arginine residue limits this exchange to only being able to donate protons. If histidine was coordinating with another residue the ability to accept protons is lost. Histidine is also an aromatic residue. The aromatic side chain in histidine could have participated in pi-pi stacking with another residue as well. The change in electrostatic interactions can reduce the stability of the protein if that interaction was essential in a series of inter- or intramolecular interactions on the extracellular region of ENaC.

Aromatic residues interactions can have a role in secondary structure stabilization by way of multiple points of interactions (30). The mutation of one aromatic ring can change a neighboring interaction. The guanidium group also can result in difference in charge distribution. Whereas, histidine has the flexibility to donate or accept electrons arginine reduces this flexibility.

In the placement of these mutations in the ENaC structure both were localized in the extracellular loop (Fig 21). The F165L mutation is in the Alpha-2 helix in the finger region of the extracellular loop (Fig 21). The H235R mutation is in the Beta-2 sheet in the beta ball of the extracellular loop (Fig 21).

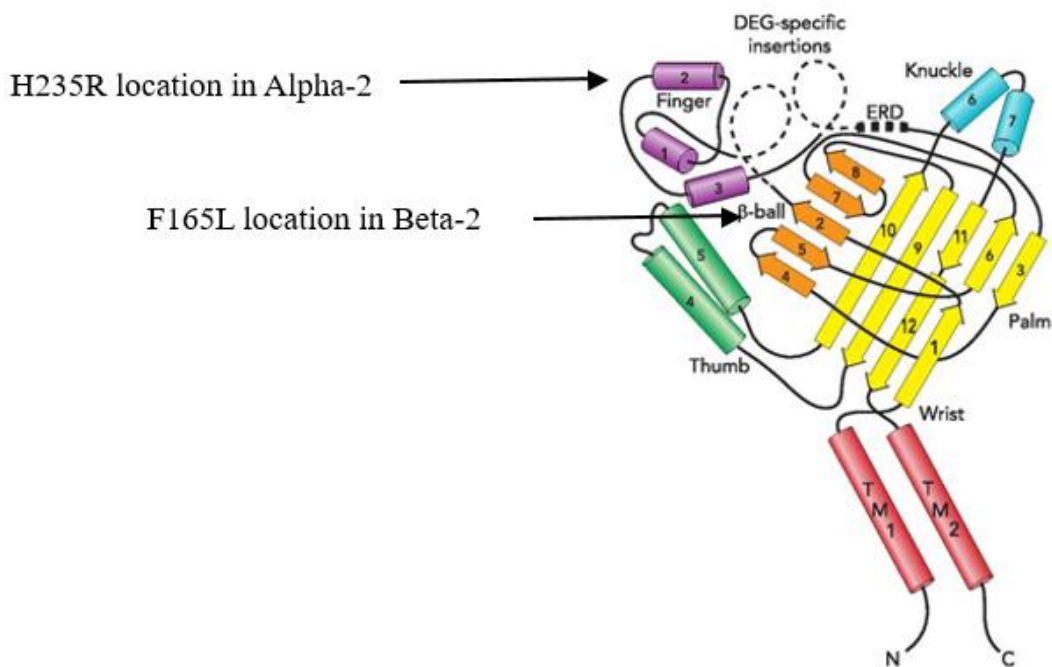


**Fig 21: Mutations in Beta mutant 1 in the Extracellular Loop Secondary Structure.** Mutations found in Beta mutant 1 are pointed out on a cartoon depiction of the secondary structure of an ENaC subunit. (10)

To visualize the localization of ENaC in the yeast system cells were prepared for slides and immunofluorescence (28). Fixed cells were stained overnight with a Myc tag antibody (1:100) overnight at room temperature. The use of the epitope antibody was to tag the epitope sequence that would have been cloned on the protein channel. The fixed cells were also stained with Alexa Flour 488 as the fluorophore. Cells were visualized on a confocal microscope at 60X oil immersion (Fig 22). Because of the size of yeast cells (2-4  $\mu\text{m}$ ) it was difficult to see exactly the localization of the mutant ENaC channel in Beta mutant 1. Future studies include localization of ENaC using confocal microscopy using a higher objective lens.

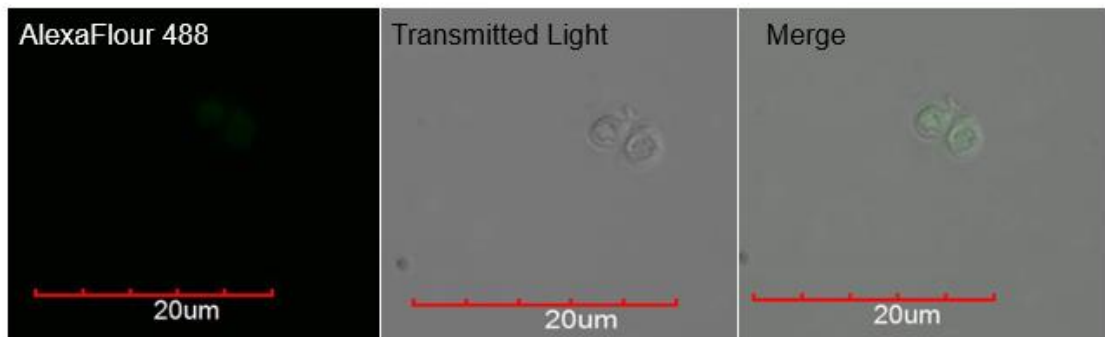


**Figure 22: Confocal Microscopy of Beta mutant 1 in BY4742 cells.** Cells were incubated overnight with anti-c-myc peroxidase, (Roche Diagnostics, Indianapolis, IN) overnight at room temperature. The fluorescent probe was the Alexaflour™ 488 goat anti-mouse IgG H+L (Life Technologies Corp. Eugene, OR). Cells were visualized on a FV1000 Confocal Microscope at 60X immersed in oil.

#### IV. CONCLUSIONS

With cardiovascular disease on the rise it is still vital to understand the assembly of ion channels that can be targeted for therapeutic treatment. It is essential to continue studying the regulation of ENaC because of the rate-limiting role in sodium reabsorption. In this study, a mutational library was created as a way to quickly screen for critical residues. The results of the salt-sensitivity assay did show phenotypic trend differences in the mutants compared to wild-type. Upon sequence analysis only one of the  $\beta$ ENaC mutants actually had missense mutations. Why did the other mutants appear to cause a phenotypic difference but the genetic code remained the same? Cloning of the PCR product into the vector could have resulted in the actual yeast model system behaving differently. A way to verify this is to clone the pESC-LEU  $\beta\gamma$  ENaC WT plasmid the same way the mutant and digested vector was recombined in yeast.

In Beta mutant 1 there were two mutations identified (Table 6). The mutations both resulted in the replacement of an aromatic residue (Table 6). Aromatic side chains are able to interact in several ways such as hydrogen bonding, pi-pi stacking, or Van der Waals forces. These residues could have been interacting with intra- or intermolecular residues. If the interaction was with a neighboring subunit then the stability of the formed protein can be manipulated. If the orientation of the extracellular loop is fixed because of the bulky aromatic residue then the loss of rigidity may have shifted the orientation.

Further analysis of beta mutant 1 is needed for clearer evidence to decide if phenylalanine and histidine are critical residues. Measuring the amount of protein expressed could provide more insight on if the expression has changed. If not, did the half-life of the protein change because the reduction of stability? Also, continuing effort

of localization of ENaC in Beta mutant 1 samples will answer if ENaC is being sent to the cytosol for degradation as a method of quality control.

## WORKS CITED

1. Blood Volume. Retrieved from <http://www.cvphysiology.com/Blood%20Pressure/BP025.htm>
2. Blood Water Homeostasis or Osmoregulation. Retrieved from <http://homeostasisinhumans.weebly.com/osmoregulation.html>
3. Regulation of Na<sup>+</sup> Balance. Retrieved from <https://courses.washington.edu/conj/bess/sodium/sodium.htm>
4. What is Aldosterone? Retrieved from <http://www.hormone.org/hormones-and-health/what-do-hormones-do/what-does-aldosterone-do>
5. Cardiovascular disease. Retrieved from [http://www.who.int/cardiovascular\\_diseases/en](http://www.who.int/cardiovascular_diseases/en)
6. Teiwes, J., & Toto, R. D. (2007). Epithelial sodium channel inhibition in cardiovascular disease. A potential role for amiloride. *Am J Hypertens*, 20(1), 109-117. doi:10.1016/j.amjhyper.2006.05.022
7. Kashlan, O. B., & Kleyman, T. R. (2011). ENaC structure and function in the wake of a resolved structure of a family member. *American Journal of Physiology - Renal Physiology*, 301(4), F684–F696. <http://doi.org/10.1152/ajprenal.00259.2011>
8. Jasti, J., Furukawa, H., Gonzales, E. B., & Gouaux, E. (2007). Structure of acid-sensing ion channel 1 at 1.9 Å resolution and low pH. *Nature*, 449(7160), 316-323. doi:10.1038/nature06163
9. Schild, L., Lu, Y., Gautschi, I., Schneeberger, E., Lifton, R. P., & Rossier, B. C. (1996). Identification of a PY motif in the epithelial Na channel subunits as a target sequence for mutations causing channel activation found in Liddle syndrome. *The EMBO Journal*, 15(10), 2381–2387.
10. Eastwood, A. L., & Goodman, M. B. (2012). Insight into DEG/ENaC channel gating from genetics and structure. *Physiology (Bethesda)*, 27(5), 282-290. doi:10.1152/physiol.00006.2012
11. Shobair, M., Dagliyan, O., Kota, P., Dang, Y. L., He, H., Stutts, M. J., & Dokholyan, N. V. (2016). Gain-of-Function Mutation W493R in the Epithelial Sodium Channel Allosterically Reconfigures Intersubunit Coupling. *Journal of Biological Chemistry*, 291(8), 3682-3692. doi:10.1074/jbc.M115.678052
12. Collier, D. M., Tomkovicz, V. R., Peterson, Z. J., Benson, C. J., & Snyder, P. M. (2014). Intersubunit conformational changes mediate epithelial sodium channel gating. *J Gen Physiol*, 144(4), 337-348. doi:10.1085/jgp.201411208
13. Mukherjee, A., Mueller, G. M., Kinlough, C. L., Sheng, N., Wang, Z., Mustafa, S. A., . . . Hughey, R. P. (2014). Cysteine Palmitoylation of the Gamma Subunit Has A Dominant Role in Modulating Activity of the Epithelial Sodium Channel. *The Journal of Biological Chemistry*, 289(20), 10.
14. JC, A. (2015). Nedd4-2 regulation of voltage-gated ion channels: an update on structure–function relationships and the pathophysiological consequences of dysfunction. *Journal of Receptor, Ligand and Channel Research*, 2015(8), 53-60.
15. Bhalla, V., & Hallows, K. R. (2008). Mechanisms of ENaC regulation and clinical implications. *J Am Soc Nephrol*, 19(10), 1845-1854. doi:10.1681/ASN.2008020225

16. Dinudom, A., Harvey, K. F., Komwatana, P., Jolliffe, C. N., Young, J. A., Kumar, S., & Cook, D. I. (2001). Roles of the C termini of alpha -, beta -, and gamma - subunits of epithelial Na<sup>+</sup> channels (ENaC) in regulating ENaC and mediating its inhibition by cytosolic Na<sup>+</sup>. *Journal of Biological Chemistry*, 276(17), 13744-13749. doi:10.1074/jbc.M011273200
17. Staub, O., Gautschi, I., Ishikawa, T., Breitschopf, K., Ciechanover, A., Schild, L., & Rotin, D. (1997). Regulation of stability and function of the epithelial Na<sup>+</sup> channel (ENaC) by ubiquitination. *EMBO J*, 16(21), 6325-6336. doi:10.1093/emboj/16.21.6325
18. Butterworth, M. B. (2010). Regulation of the epithelial sodium channel (ENaC) by membrane trafficking. *Biochim Biophys Acta*, 1802(12), 1166-1177. doi:10.1016/j.bbadis.2010.03.010
19. Soundararajan, R., Pearce, D., Hughey, R. P., & Kleyman, T. R. (2010). Role of epithelial sodium channels and their regulators in hypertension. *Journal of Biological Chemistry*, 285(40), 30363-30369. doi:10.1074/jbc.R110.155341
20. Frindt, G., & Palmer, L. G. (2009). Surface expression of sodium channels and transporters in rat kidney: effects of dietary sodium. *Am J Physiol Renal Physiol*, 297(5), F1249-1255. doi:10.1152/ajprenal.00401.2009
21. Haerteis, S., Krappitz, M., Diakov, A., Krappitz, A., Rauh, R., & Korbmacher, C. (2012). Plasmin and chymotrypsin have distinct preferences for channel activating cleavage sites in the gamma subunit of the human epithelial sodium channel. *J Gen Physiol*, 140(4), 375-389. doi:10.1085/jgp.201110763
22. Yang, K. Q., Lu, C. X., Xiao, Y., Liu, Y. X., Jiang, X. J., Zhang, X., & Zhou, X. L. (2015). A novel frameshift mutation of epithelial sodium channel beta-subunit leads to Liddle syndrome in an isolated case. *Clin Endocrinol (Oxf)*, 82(4), 611-614. doi:10.1111/cen.12650
23. Edelheit, O., Hanukoglu, I., Shriki, Y., Tfilin, M., Dascal, N., Gillis, D., & Hanukoglu, A. (2010). Truncated beta epithelial sodium channel (ENaC) subunits responsible for multi-system pseudohypoaldosteronism support partial activity of ENaC. *Journal of Steroid Biochemistry and Molecular Biology*, 119(1-2), 84-88. doi:10.1016/j.jsbmb.2010.01.002
24. Kucher, V., Boiko, N., Pochynyuk, O., & Stockand, J. D. (2011). Voltage-dependent gating underlies loss of ENaC function in Pseudohypoaldosteronism type 1. *Biophys J*, 100(8), 1930-1939. doi:10.1016/j.bpj.2011.02.046
25. Mora-Lopez, F., Bernal-Quiros, M., Lechuga-Sancho, A. M., Lechuga-Campoy, J. L., Hernandez-Trujillo, N., & Nieto, A. (2012). Novel mutation in the epithelial sodium channel causing type I pseudohypoaldosteronism in a patient misdiagnosed with cystic fibrosis. *Eur J Pediatr*, 171(6), 997-1000. doi:10.1007/s00431-012-1697-5
26. Okonkwo, A. (2016). *Uncovering the Critical Amino Acids in the Beta Subunit of the Epithelial Sodium Channel (ENaC)*. (Master of Science), Texas State University, San Marcos, TX.
27. Ybanez, R. (2009). *The Development of a Quick Screen in Yeast for Functional Epithelial Sodium Channels*. (Master of Science Msc. Thesis), Texas State University.

28. Atkin, Audrey L. (1999). Preparation of Yeast cells for Microscopy. *Methods in Molecular Biology*, 122, 1231-139.
29. Whistenant, Ty E. (2011). *Identification of Residues Critical to Epithelial Sodium Channel Assembly*. (Master of Science). Texas State University, San Marcos, TX
30. Anjana, Ramnath, Vaishnavi, Marthandan Kirti, Sherlin, Durairaj, Kumar, Surapaneni Pavan, Naveen, Kora, Kanth, & Sekar, Kanagaraj. (2012). Aromatic-aromatic interactions in structures of proteins and protein-DNA complexes: a study based on orientation and distance. *Bioinformation*, 8 (24), 1220-1224. doi:10.6026/97320630081220.